

Quantifying Percent-Cover in Prescott National Forest, Arizona;
Through the Integration of Landsat Imagery, Vegetation Indices, and Spatial Transformations

by

Tracy Lynn Schirmang

A Thesis Presented in Partial Fulfillment
of the Requirements for the Degree
Master of Arts

Approved February 2012 by the
Graduate Supervisory Committee:

Patricia L. Fall, Co-Chair
Soe W. Myint, Co-Chair
Anthony J. Brazel

ARIZONA STATE UNIVERSITY

May 2012

ABSTRACT

Accurate characterization of forest canopy cover from satellite imagery hinges on the development of a model that considers the level of detail achieved by field methods. With the improved precision of both optical sensors and various spatial techniques, models built to extract forest structure attributes have become increasingly robust, yet many still fail to address some of the most important characteristics of a forest stand's intricate make-up. The objective of this study, therefore, was to address canopy cover from the ground, up. To assess canopy cover in the field, a vertical densitometer was used to acquire a total of 2,160 percent-cover readings from 30 randomly located triangular plots within a 6.94 km² study area in the central highlands of the Bradshaw Ranger District, Prescott National Forest, Arizona. Categorized by species with the largest overall percentage of cover observations (*Pinus ponderosa*, *Populus tremuloides*, and *Quercus gambelii*), three datasets were created to assess the predictability of coniferous, deciduous, and mixed (coniferous and deciduous) canopies. Landsat-TM 5 imagery was processed using six spectral enhancement algorithms (PCA, TCT, NDVI, EVI, RVI, SAVI) and three local windows (3x3, 5x5, 7x7) to extract and assess the various ways in which these data were expressed in the imagery, and from those expressions, develop a model that predicted percent-cover for the entire study area. Generally, modeled cover estimates exceeded actual cover, over predicting percent-cover by a margin of 9-13%. Models predicted percent-cover more accurately when treated with a 3x3 local window than those treated with 5x5 and 7x7 local windows. In addition, the performance of models defined by the principal components of three vegetation indices (NDVI, EVI, RVI) were superior to those defined by the principal components of all four (NDVI, EVI, RVI, SAVI), as well as the principal and tasseled cap components of all multispectral bands (bands 123457). Models designed to predict mixed and coniferous percent-cover were more accurate than deciduous models.

ACKNOWLEDGEMENTS

I would like to thank Dr. Soe Myint, Dr. Patricia Fall, Dr. Anthony Brazel, the American Society for Photogrammetry and Remote Sensing, Nancy Peterson, Aaron Cumashot, JoAnna Klinge, the National Forest Service, family and friends. Your support was essential and I remain grateful for your advice, encouragement, and contributions.

TABLE OF CONTENTS

	Page
LIST OF TABLES	v
LIST OF FIGURES.....	vi
CHAPTER	
1 INTRODUCTION	1
1.1 Rationale.....	1
1.2 Previous Studies	2
1.3 Research Design.....	3
1.4 Research Questions	4
2 STUDY AREA.....	5
2.1 Landscape	5
2.2 Phytogeography.....	5
3 PREDICTING PERCENT-COVER.....	7
3.1 Methods Overview	7
3.2 Field Procedures	7
3.2.1 Sampling Scheme and Transect Configuration	7
3.2.2 Cover Estimates.....	8
3.2.3 Plot Composition Estimates	11
3.3 Digital Analysis	12
3.3.1 Data Acquisition and Pre-Processing	12
3.3.2 Band Transformations	15
3.3.3 Pre-Model Statistical Analyses	19
3.3.4 Model Construction.....	19
3.3.5 Predicting Canopy Cover	22
3.3.6 Model Accuracy	22
4 RESULTS.....	24
4.1 Pre-Model Statistical Analyses	24

4.2 Post-Model Statistical Analyses.....	27
4.2.1 Correlation and Post-Model MLR.....	27
4.2.2 Residual Variance	34
5 DISCUSSION AND CONCLUSION.....	38
5.1 Spectral Response to Landscape Dynamics	38
5.1.1 Influence of Forest Structure on Data.....	38
5.1.2 Regional Influence on Data.....	39
5.2 Examination of Techniques and Procedures	39
5.2.1 Data Acquisition.....	40
5.2.2 Normalizing Cover.....	40
5.3 Conclusions	41
REFERENCES.....	42

LIST OF TABLES

Table	Page
3.1 Study area plot descriptions.....	9
3.2 Accuracy assessment of classified orthophoto.....	13
3.3 Landsat-5 TM Band transformation algorithms	15
3.4 Mixed cover model equations	20
3.5 Coniferous cover model equations	21
3.6 Deciduous cover model equations	22
4.1 Pre-model MLR results for mixed cover	25
4.2 Pre-model MLR results for coniferous cover	26
4.3 Pre-model MLR results for deciduous cover	27
4.4 Post-model correlation coefficients	31
4.5 Post-model MLR results and p-value figures for final mixed cover models	34
4.6 Post-model MLR results and p-value figures for final coniferous-cover models	34
4.7 Residual variance and RMSE figures for final mixed-cover models	35
4.8 Residual variance and RMSE figures for final coniferous-cover models.....	35

LIST OF FIGURES

Figure		Page
2.1	Study area and plot distribution map.....	6
3.1	Plot construction and transect configuration	8
3.2	Plot composition estimate map (P4), used to derive birds-eye relevé in the field.	11
3.3	Digitized plot P4 polygon over Landsat-5 TM imagery	12
3.4	Orthophoto transformations	14
3.5	Example of 3x3 local window used to decrease locational error	16
3.6	Band transformation decision-tree	17
3.7	Transformation outputs used for preliminary MLR	18
4.1	Percent-cover model outputs for mixed-cover	28
4.2	Percent-cover model outputs for coniferous-cover	29
4.3	Percent-cover model outputs for deciduous-cover	30
4.4	Post-model MLR vegetation fractions for mixed-cover	32
4.5	Post-model MLR vegetation fractions for coniferous-cover	33
4.6	Residual variance and RMSE figures for final mixed-cover models	36
4.7	Residual variance and RMSE figures for final coniferous-cover models	37

CHAPTER 1

INTRODUCTION

1.1 Rationale

The quantification of forest canopy cover by satellite imagery is of great relevance to a wide variety of applications in the physical science community. Defined as the “proportion of forest floor covered by the vertical projection of tree crowns” (Jennings et al. 1999), tree canopy involves the collective cover and arrangement of single or multiple tree crowns; the space under which light has been intercepted by foliage. Where the sun’s radiation is not trapped by leaves, pockets of light penetrate the vertical space between canopies, making the irregular distribution of leaves within heterogeneous canopies particularly difficult to distinguish from a distance far above.

In recent years models of forest structure attributes have become increasingly robust. However, despite the improved precision of both optical sensors and various spatial techniques, many models have difficulty incorporating some of the most important characteristics of a forest stand’s intricate make-up. The objective of this study, therefore, is to offer a model developed from the ground, up; to generate a Landsat-5 TM model that predicts percent-cover on a pixel-by-pixel basis via training data produced through a field assessment of canopy cover in Prescott National Forest, Arizona.

This research examines the ability of certain remote sensing applications to quantify ecological relationships and creates a vegetation model that incorporates features undetectable with 30 meter resolution satellite imaging. Prescott National Forest’s Bradshaw Ranger District offers a heterogeneous landscape with diverse cover types as the basis for this model, in which highly variable spatial and spectral ecology provide an ideal setting to test the quality of the model against. Two of these cover types are especially important to the region: a rare and ancient colony of quaking aspen, and a population of Ponderosa pine threatened recently (beginning in 2002) by bark beetles (*Dendroctonus valens* and *Ips lecontei*) (Shalau 2003), which are experiencing a 30% mortality rate today (USFS 2011).

1.2 Previous Studies

Many studies have focused on the quantification of canopy cover through satellite imagery (e.g., Franklin et al. 1991, Salvador and Pons 1998, Huang et al. 2001, Huang 2006, Carreiras et al. 2006, Smith et al. 2010). Though satellite imagery is suggested to be a key solution to issues that restrain canopy cover research, a great deal of groundwork has been laid prior to the use of remote sensing (Stumpf 1993). While some imagery-focused studies do not include a field assessment (Carreiras et al. 2005, Huang et al. 2001), tandem use of ground based and remotely sensed investigations are ideal. In this study, I use forest stand cover observations, compare these data to cover estimates provided by satellite imagery, and then predict percent-cover through the use of several vegetation indices and spatial transformations.

One particular difficulty in remote sensing is the ability to accurately assess deciduous forest percent-cover, as the complex structure and layered nature of deciduous species is more common on steep topography, and creates shadowing, low spectral signals, understory-mixed spectra, as well as confuses many satellite-based textural analyses, such as tasseled cap transformations (Crist and Cicone 1986, Franklin et al. 1991, Wulder 1998, Dymond et al. 2002, Carreiras et al. 2005). In addition, deciduous canopies are affected by wind in ways that coniferous canopies are not, as winds may overturn and expose the abaxial (lower) surface of deciduous foliage, creating problematic variability in the spectra of deciduous forest stands (Wolter et al. 1995). In this study, therefore, I explore the spectral expression of multiple vegetation indices at several spatial scales within deciduous stands, coniferous stands, and mixed coniferous and deciduous stands to learn more about predicting canopy cover in a heterogeneous forest landscape.

Several notable works have provided a reliable foundation. One of the most relevant studies, Carreiras et al. (2006), which looked at the predictability of canopy cover in a heterogeneous evergreen oak woodland with individual multispectral Landsat TM bands, several individual vegetation indices (Normalized Difference (NDVI), Soil-Adjusted (SAVI), Modified Soil-Adjusted (MSAVI), Green Normalized Difference (GNDVI), Atmospherically-Resistant (ARVI), V15, and V17), and tasseled cap transformations, found that the three most accurate models used bands 3,4,5, and 7 ($r^2 = 0.74$), NDVI ($r^2 = 0.72$), and tasseled cap transformation

components ($r^2 = 0.70$). It is my study's intent, however, to use *in situ* cover observations, explore how to translate those figures from satellite imagery, and use such translations to predict cover.

1.3 Research Design

This study explores the relationship between canopy cover, Landsat imagery, and nine application transformations. Transformed outputs are calibrated on the basis of a detailed *in situ* assessment of heterogeneous canopies to develop a reliable model for predicting coniferous, deciduous, and mixed (coniferous and deciduous) canopy cover percentages on a pixel-by-pixel basis. To predict canopy cover by means of Landsat imagery, the facility of two spectral applications (principal component and tasseled cap analyses), four vegetation indices, and three local windows are explored.

Canopy cover was assessed in the field using a vertical densitometer to acquire 2,160 readings of canopy cover percentages between September 2008 and January 2009 from 30 randomly located triangular plots within the study area. Categorized by those species with the largest overall percentage of canopy cover observations ("P" for *Pinus ponderosa*, "A" for *Populus tremuloides*, and "K" for *Quercus gambelii*), three datasets were created to assess the predictability of coniferous (*P. ponderosa*), deciduous (*P. tremuloides* and *Q. gambelii*) and mixed (coniferous and deciduous) canopies. A Landsat-5 TM image (path/row 37/36, acquired 19 May 2008) was processed using multiple applications to extract and assess the various ways in which these data are expressed in the imagery, and from those expressions, to develop a model that predicts canopy cover for the entire study area.

Six spectral enhancement algorithms, Principal Component Analysis (PCA), Tasseled Cap Transformation (TCT), Normalized Differentiation Vegetation Index (NDVI), Enhanced Vegetation Index (EVI), Simple Ratio Vegetation Index (RVI), and Soil-Adjusted Vegetation Index (SAVI), were used to optimize the imagery for vegetation, with specific attention to canopy cover (which also required spectral enhancements that not only highlighted vegetation, but also minimized atmospheric and soil background noise). To address the spatial arrangement and local variability of pixels within the study area, three local windows were applied to the outputs produced by the spectral enhancements above. The transformed outputs were stacked as layers

and joined into one file to extract the digital values of each pixel of interest (i.e., those that intersected a plot), thereby preparing the data for a preliminary multiple linear regression analysis.

Three sets of preliminary multiple linear regression analyses use the datasets of coniferous, deciduous and mixed (coniferous and deciduous) cover to consider which of the nine transformations (PCA, TCT, NDVI, EVI, RVI, SAVI, and 3x3, 5x5, 7x7 local windows) reflect field-drawn average canopy cover percentages most accurately. These analyses compare average canopy cover values for all plots (P1-P17, A1-A6, and K1-K7), coniferous plots (P1-P17) and deciduous plots (A1-A6, K1-K7) to the digital values for the pixels that intersect each plot. The resulting intercept and regression coefficients for the most accurate transformations (or transformation combinations) are used to build 54 final models (18 coniferous models, 18 deciduous models, and 18 mixed-cover models) which, when applied to the imagery, predict canopy cover percentages on a pixel-by-pixel basis for the entire study area. Thus, the objectives of this study were threefold.

1.4 Research Questions

1. Are the principal components of different band combinations (b12345, b123457) composite bands (TC) and/or vegetation indices (NDVI, EVI, RVI, SAVI) an effective way to predict percent-cover?
2. Which window size (3x3, 5x5, 7x7) is the optimal size for predicting percent-cover?
3. Which forest-type (mixed, coniferous, deciduous) is percent-cover predicted with the highest accuracy?

CHAPTER 2

STUDY AREA

2.1 Study Area

2.1.1 Landscape

Prescott National Forest is comprised of a unique mixture of phytogeographic conditions that stretch roughly 5,000 km² across the state's central highlands (USFS 2006). From the northern reaches of the Sonoran Desert to the montane conifer forests of Arizona's interior woodlands, the Prescott National Forest consists of elevations between 800-2400 m and thus accommodates a wide variety of vegetation within its boundaries (USFS 2006). Today, the forest is divided into two sections (west and east), three ranger districts (Chino Valley, Verde, and Bradshaw), and eight wildlife areas (USFS 2006). Originally established in 1898 to protect the area's watershed and timberlands, President McKinley first reserved a portion of what today falls within the northern stretch of the Bradshaw Ranger District (USFS 2006). Straddling the south fork of Aspen Creek, the study area (see Figure 3.1) is nestled within McKinley's primary boundaries, less than 16 km southeast of the town of Prescott, Arizona.

2.1.2 Phytogeography

Extending across an elevational range of 1900-2150 m, the 6.94 km² study area contains a wide variety of plant life. Sustained by a microclimate attributed to Aspen Creek's highland descent from the Sierra Prieta Mountains, an ancient colony of quaking aspen (*Populus tremuloides*) is hypothesized to have persisted since the Pleistocene (Ryberg 2005). The area's vegetation is predominantly alligator juniper (*Juniperus deppeana*) – some of which are up to 1800 years old – boxelder (*Acer negundo*), cottonwood (*Populus fremontii*), elm (*Ulmus pumila*), oak (*Quercus gambelii*, *Q. turbinella*, and *Q. arizonica*), ponderosa pine (*Pinus ponderosa*), walnut (*Juglans major*), and willow (*Salix* spp.) (Crowin 2004, Ryberg 2005). A variety of herbaceous plants, such as alfalfa (*Medicago sativa*), lupine (*Lupinus* spp.), mint (*Mentha arvensis*), toadflax (*Linaria dalmatica*), wild rose (*Rosa wodsii*), and shrubs including buckthorn (*Rhamnus* spp.), ceanothus (*Ceanothus* spp.), manzanita (*Arctostaphylos* spp.), and snowberry (*Symphoricarpos* spp.), also are present (Corwin 2004, SEINet 2011, Ryberg 2005). The study area captures a sampling of mixed evergreen and deciduous forest stands found in the mountainous southwestern United States. Characterizing this area's stand attributes from satellite

imagery will refine our understanding of vegetation in this study area and should prove similarly useful for other southwestern landscapes.

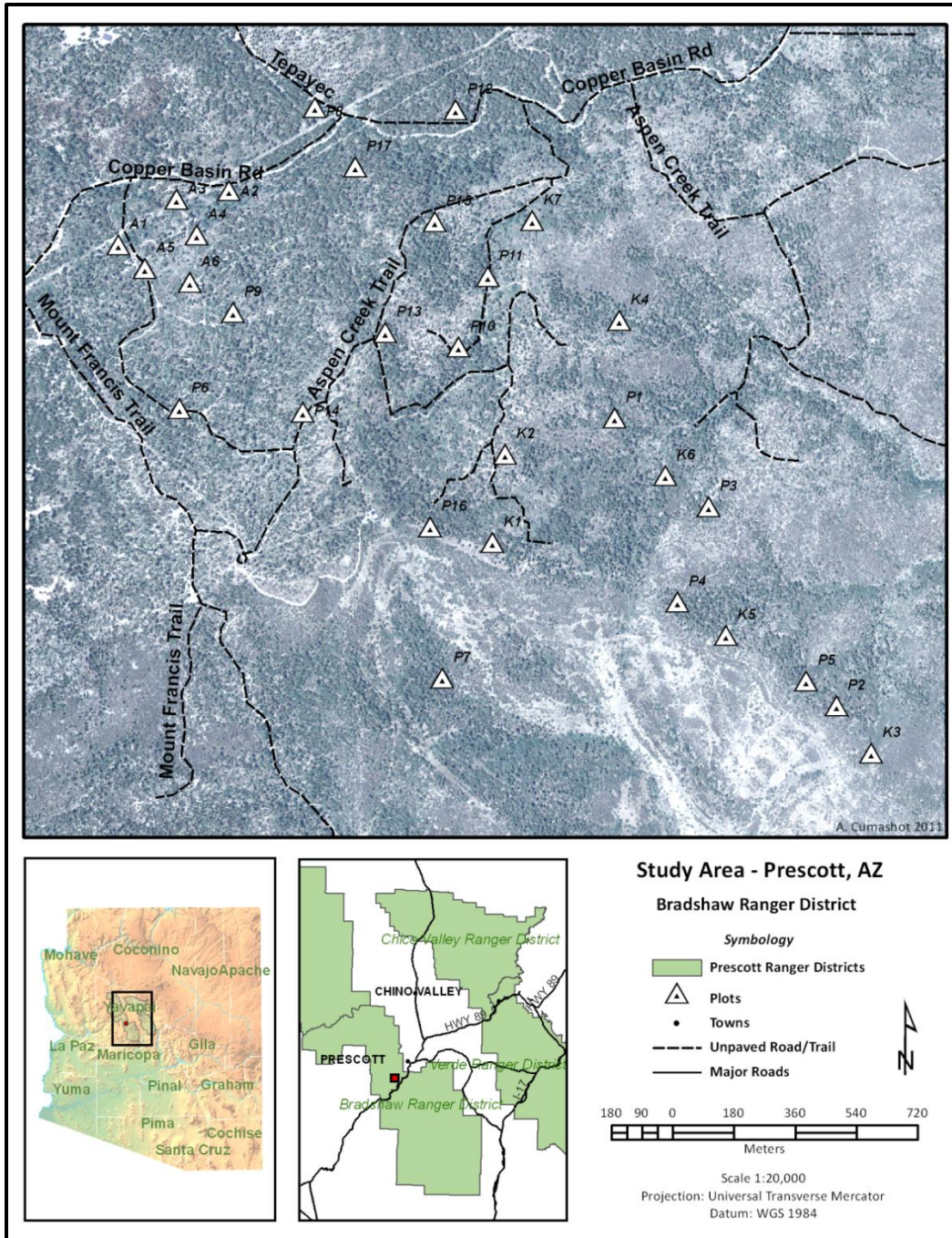


Figure 2.1 Study area and plot distribution map, situated southeast of Prescott, Arizona within Prescott National Forest's Bradshaw Ranger District.

CHAPTER 3

PREDICTING PERCENT-COVER

3.1 Methods Overview

Utilizing Landsat-5 TM imagery to explore canopy cover, the facility of four vegetation indices, two sets of composite bands, and three moving windows were explored on the basis of a detailed *in situ* assessment of canopy cover. Ultimately, the facility of six spectral transformations (two composite transformations and four vegetation indices) and three spatial arrangements (three moving windows) were examined to develop a reliable model for predicting coniferous, deciduous, and mixed (coniferous and deciduous) percent-cover on a pixel-by-pixel basis. This chapter summarizes the techniques and procedures of both the field and digital analyses.

3.2 Field Procedures

3.2.1 Sampling Scheme and Transect Configuration

Vegetation field data were acquired from 30 triangular plots located randomly within the 6.94 km² study area (see Figure 2.1). Each plot was defined by three transects of equal length (approximately 44 m) (adhering to methods of Stumpf 1993). Transect 3, positioned at the base of each plot, was aligned on an east-west axis; the top of each plot, where transects 1 and 2 intersected, pointed due north (see Figure 3.1). Each plot adheres to the following physiographic conditions:

- a) The slope within each plot is less than 20%, to ensure adequate view and illumination angles from the imagery.
- b) The boundary of each plot intercepts no less than two trees of interest, given that this study evaluates canopy cover.
- c) Each plot lies at least 50 m from any other plot, to avoid overlapping plot-pixel coverage.

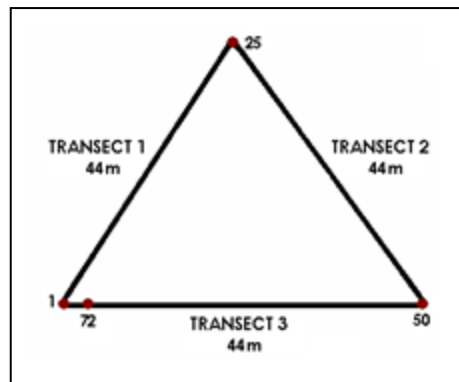


Figure 3.1 Plot construction and transect configuration, consisting of 44 m transects and 72 sampling points.

3.2.2 Cover Estimates

Cover estimates were generated with a vertical densitometer, based on measurements taken at sampling points located at 1.8 meter intervals along each transect. The boundary of each plot therefore consists of 72 total canopy cover sampling points (24 points per transect; along each side of the triangle). These methods also stem from Stumpf’s (1993) evaluation of densitometer-based techniques. At each point, the vertical densitometer was used to determine the percentage of ponderosa pine (*Pinus ponderosa*), quaking aspen (*Populus tremuloides*), and Gambel oak (*Quercus gambelii*) canopy cover directly overhead by estimating what percentage of the instrument’s field of view was obstructed. All observations of canopy cover by species, excluding those listed above were classified as “other.” The species of each observed canopy was recorded, as were notes concerning the observed tree’s position in relation to the plot and nearest sampling point (e.g., whether the trunk of the observed tree was situated within or outside the triangular plot). If multiple species or multiple layers of vegetation were encountered, their collective cover was recorded, and each species as well as their layered arrangement was documented. All juvenile trees less than two meters in height and understory vegetation were noted, but not included in canopy estimates. Based on these data, each plot was categorized as “P” for *P. ponderosa*, “A” for *P. tremuloides* or “K” for *Q. gambelii* according to ubiquity, determined by the dominance of ponderosa, aspen, or oak densitometer readings (see Table 3.1 and Figure 2.1).

Table 3.1 Estimated canopy cover for the 30 sample plots utilized in this study, including plot category, number, elevation, latitude, longitude, species ubiquity (based on the highest relative percentage of A, K, or P readings per plot), and plot composition relevé (derived from sketched maps of estimated birds-eye cover, discussed below in the following section). Plots A1-6 were dominated by quaking aspen, plots K1-7 were dominated by Gambel oak, and plots P1-17 were dominated by ponderosa pine on the basis of their ubiquity (the number of points at which the dominant species is present divided by 72, which is expressed as a percentage).

Plot ID	Elevation (m)	Latitude (ddmmss.sssss)	Longitude (dddmmss.sssss)	Ubiquity (%) ^a
A1	2030	34 29 48.75854	-112 32 32.06053	59%
	Mixed ^b (40%), <i>P. tremuloides</i> (38%), <i>P. ponderosa</i> (10%), other tree (5%), Forest Rd. 9402D (5%), <i>Q. gambelii</i> (2%)			
A2	2007	34 29 54.29007	-112 32 19.44907	61%
	<i>P. tremuloides</i> (30%), shrub (40%), leaf-litter (25%), herbacious (10%), Aspen Creek (8%), woody debris (5%), other tree (7%)			
A3	2012	34 29 53.33927	-112 32 25.34225	66%
	Mixed (54%), <i>P. tremuloides</i> (20%), powerline clearing (10%), <i>P. ponderosa</i> (5%), boulder (5%), <i>J. deppeana</i> (4%), exposed soil (2%)			
A4	2012	34 29 49.94199	-112 32 23.17233	72%
	<i>P. tremuloides</i> (61%), shrub, herbacious (20%), leaf-litter, exposed soil (10%), <i>P. ponderosa</i> (1%)			
A5	2047	34 29 46.68867	-112 32 28.88581	80%
	<i>P. tremuloides</i> (40%), mixed (30%), Forest Rd. 9402D (10%), boulder (6%), <i>J. deppeana</i> (3%) other tree (3%), <i>P. ponderosa</i> (3%), <i>Arctostaphylos</i> spp. (3%), <i>Q. gambelii</i> (2%)			
A6	2038	34 29 45.38970	-112 32 23.78456	85%
	<i>P. tremuloides</i> (65%), mixed (15%), <i>P. ponderosa</i> (8%), shrub (5%), boulder (5%), woody debris (2%)			
K1	2096	34 29 20.93580	-112 31 48.49225	48%
	<i>P. ponderosa</i> (35%), <i>Q. gambelii</i> (25%), woody debris, shrub (15%), leaf-litter (14%), exposed soil, gravel (5%), herbacious (5%), <i>J. deppeana</i> (1%)			
K2	2057	34 29 29.49046	-112 31 47.10973	48%
	Mixed (40%), <i>Q. gambelii</i> (20%), <i>P. ponderosa</i> (15%), shrub (10%), woody debris (10%), <i>Q. terbinella</i> (5%)			
K3	2000	34 29 01.52275	-112 31 04.38858	53%
	<i>Q. gambelii</i> (50%), leaf-litter, woody debris (20%), <i>P. ponderosa</i> (10%), <i>J. deppeana</i> (10%), exposed soil, gravel (7%), shrub (3%)			
K4	1975	34 29 42.47563	-112 31 34.09496	62%
	Shrub, leaf-litter, woody debris (46%), <i>Q. gambelii</i> (30%), <i>P. ponderosa</i> (20%), exposed soil (4%)			
K5	2003	34 29 12.55891	-112 31 21.38710	68%
	<i>Q. gambelii</i> (30%), <i>P. ponderosa</i> (15%), leaf-litter (15%), woody debris (15%), shrub (14%), <i>J. deppeana</i> (6%), herbacious (5%)			

Table 3.1 continued

Plot ID	Elevation (m)	Latitude (ddmmss.sssss)	Longitude (dddmmss.sssss)	Ubiquity (%)
K6	1983	34 29 27.65992	-112 31 28.66952	82%
	<i>Q. gambelii</i> (37%), shrub, leaf-litter (30%), exposed soil, cobble, gravel (15%), herbacious (10%), woody debris (5%), <i>P. ponderosa</i> (3%)			
K7	1992	34 29 51.80873	-112 31 44.42979	87%
	<i>Q. gambelii</i> (42%), shrub (25%), leaf-litter, woody debris (20%), <i>P. ponderosa</i> (8%), exposed soil, gravel (5%)			
P1	1984	34 29 33.13789	-112 31 34.50308	45%
	<i>Q. gambelii</i> (45%), <i>P. ponderosa</i> (20%), leaf-litter (15%), woody debris (5%), herbacious (5%), other tree (5%), boulder (3%), shrub (2%)			
P2	1998	34 29 05.88617	-112 31 08.51528	45%
	<i>Q. gambelii</i> (50%), shrub, woody debris (26%), <i>P. ponderosa</i> (12%), leaf-litter (5%), <i>J. deppeana</i> (3%), boulder (2%), herbacious (2%)			
P3	2002	34 29 24.72363	-112 31 23.35283	50%
	<i>P. ponderosa</i> (30%), leaf-litter, boulder, herbacious (30%), <i>Q. gambelii</i> (20%), shrub (10%), woody debris (10%)			
P4	2022	34 29 15.65163	-112 31 27.17683	56%
	Mixed (45%), <i>P. ponderosa</i> (25%), <i>Q. gambelii</i> (18%), trail (5%), <i>J. deppeana</i> (5%), <i>Arctostaphylos</i> spp. (2%)			
P5	1996	34 29 8.358423	-112 31 12.00993	63%
	<i>Q. gambelii</i> (40%), <i>P. ponderosa</i> (23%), leaf-litter, woody debris (25%), boulder (5%), herbacious (5%), shrub (2%)			
P6	2068	34 29 33.36748	-112 32 24.70046	64%
	<i>P. ponderosa</i> (30%), <i>J. deppeana</i> (30%), leaf-litter (25%), shrub (7%), <i>Q. gambelii</i> (4%), woody debris (4%)			
P7	2036	34 29 07.99605	-112 31 53.97946	64%
	<i>J. deppeana</i> (30%), <i>P. ponderosa</i> (25%), leaf-litter (25%), boulder (10%), woody debris (5%), herbacious (5%)			
P8	1995	34 29 02.19090	-112 32 09.41941	71%
	<i>P. ponderosa</i> (25%), leaf-litter, woody debris (25%), herbacious (24%), <i>P. tremuloides</i> (8%), Copper Basin Rd. (8%), boulder (5%), exposed soil (5%)			
P9	2039	34 29 42.53066	-112 32 18.83111	80%
	Leaf-litter (27%), shrub (20%), herbacious (16%), <i>P. ponderosa</i> (12%), <i>Arctostaphylos</i> spp. (8%), cobble (5%), <i>Q. gambelii</i> (4%), woody debris (3%), <i>Q. turbinella</i> (2%)			
P10	2000	34 29 02.06824	-112 31 53.35106	81%
	<i>P. ponderosa</i> (65%), leaf-litter (15%), woody debris (6%), <i>Q. gambelii</i> (5%), <i>Arctostaphylos</i> spp. (5%), boulder (2%), <i>J. deppeana</i> (2%)			
P11	2018	34 29 46.29027	-112 31 49.61223	83%
	<i>P. ponderosa</i> (30%), <i>Q. gambelii</i> (15%), woody debris (15%), leaf-litter (15%), shrubs, herbacious (10%), trail (10%), creek (5%)			
P12	2048	34 29 39.69538	-112 31 52.61843	84%
	<i>P. ponderosa</i> (40%), leaf-litter, woody debris (34%), <i>Q. turbinella</i> (15%), <i>Q. gambelii</i> (4%), herbacious (3%), shrub (2%), boulder (2%)			
P13	2097	34 29 40.96823	-112 32 01.12017	84%
	Leaf-litter (20%), <i>P. ponderosa</i> (15%), herbacious (14%), other tree (11%), shrub (10%), woody debris (10%), exposed soil, gravel (10%), Aspen Creek trail (5%), <i>Q. gambelii</i> (3%), boulder (2%)			

Table 3.1 continued

Plot ID	Elevation (m)	Latitude (ddmmss.ssss)	Longitude (dddmmss.ssss)	Ubiquity (%)
P14	2087	34 29 33.28694	-112 32 10.48690	84%
<i>P. ponderosa</i> (20%), leaf-litter (20%), <i>J. deppeana</i> (15%), shrub (15%), <i>Arctostaphylos</i> spp. (8%), mixed (8%), trail (6%), <i>Q. gambelii</i> (6%), boulder (2%)				
P15	2036	34 29 51.52183	-112 31 55.65768	86%
Leaf-litter (40%), <i>P. ponderosa</i> (20%), <i>Q. gambelii</i> (8%), woody debris (8%), shrub (8%), exposed soil (5%), herbacious (5%), <i>Q. turbinella</i> (3%), boulder (3%)				
P16	2130	34 29 22.66249	-112 31 55.75701	90%
Leaf-litter, exposed soil, gravel (40%), <i>P. ponderosa</i> (30%), herbacious (20%), <i>J. deppeana</i> (5%), woody debris (5%)				
P17	2010	34 29 56.63176	-112 32 04.91624	96%
<i>P. ponderosa</i> (53%), leaf-litter (15%), shrub (10%), woody debris (10%), herbacious (4%), exposed soil, gravel (4%), boulder (4%)				

^a Relative percentage of *P. tremuloides*, *Q. gambelii*, and *P. ponderosa* readings (i.e. species-specific canopy cover readings per plot / total number of species-specific canopy cover readings per plot); ^b a heterogeneous yet even mixture of four or more cover-types within one or more areas of a plot.

3.2.3 Plot Composition Estimates

Birds-eye plot composition relevé also were created by mapping each plot's cover in the field. This technique renders the data from Table 3.1 in a vegetation sketch format (see Figure 3.2). This format provides a detailed record of each plot's physical makeup.

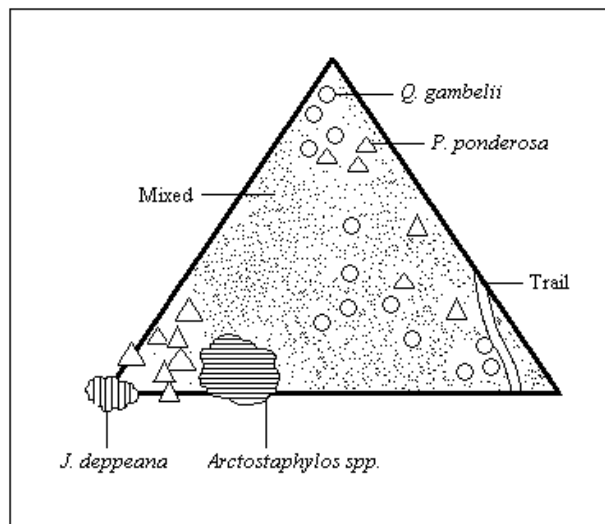


Figure 3.2 Plot composition estimate map of plot P4 (converted to digital format) used to derive birds-eye relevé in the field.

3.3 Digital Analysis

3.3.1 Data Acquisition and Pre-processing

The Landsat-5 TM image (path/row 37/36, acquired 19 May 2008) used in this study was obtained from the USGS Global Visualization Viewer (GLOVIS). A subset of all multispectral bands (bands 123457) was used to isolate the 6.94 km² study area from the Landsat-5 TM imagery. Area of interest (AOI) polygons were digitized to display each plot's specific location (see Figure 3.3) and integrate the GPS coordinates that define each of these triangular plots. The measurement tool was then used to quantify the area of each plot. Plot coverage varied, since some plots traversed 3 pixels, while others traversed 4, 5, 6 or 7 pixels. Accordingly, the plot-pixel area of overlap was quantified for each individual pixel by measuring the area of each pixel that fell within the boundaries of each plot, thereby quantifying which pixel intersected the greatest percentage of each plot. The pixels that intersected the greatest area of their respective plot were used exclusively for all further analyses, as they contained the majority of the information needed to explore the relationship between each plot's spectra and actual cover.

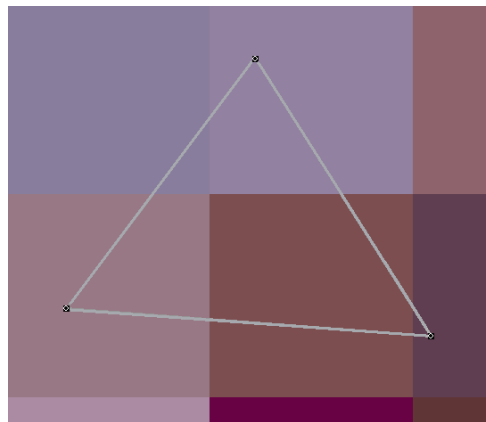


Figure 3.3 Screenshot of triangle plot (P4) position over pixels, used to determine which pixel intersected the highest percentage of a plot's total coverage.

An orthophoto of Yavapai County from the United States Department of Agriculture's (USDA) National Agriculture Imagery Program (NAIP), photographed during the 2007 growing season at 1m resolution, was used to assess the validity of the models presented in this study. A subset of the study area was used to prepare the orthophoto for this assessment. An unsupervised

classification (prepared with 100 classes, 25 iterations, and a convergence threshold of 0.97) was performed with the use of a reiterating self-organizing data analysis (ISODATA) classifier. The output was then recoded into two classes—forest and non-forest—generating a black and white output for the study area. An accuracy assessment (see Table 3.2) was performed (within the constraints of a stratified-random sampling of 200 pixels, with a minimum of 75 pixels per class). This determined the integrity of the classified output by comparing the class value (Non-forest [0] and Forest [1]) of 200 classified pixels to the original subsetted orthophoto, and generated an overall accuracy of 88%, exceeding the minimum target tolerance of 85% (Tomlinson et al. 1999).

Table 3.2 Accuracy assessment of classified orthophoto.

Class	Producer Accuracy (%)	User Accuracy (%)	Kappa Statistics
Non-forest (0)	88.4	90.0	0.77
Forest (1)	87.5	85.6	0.74
Overall Classification Accuracy (%) = 88.0			
Overall Kappa Statistics = 0.76			

Next, to minimize locational errors (between the Landsat and orthophoto imagery), two speckle suppression filters—a 31x31 mean filter and a 91x91 mean filter—were applied, producing two outputs. This approach filtered the mean pixel value of each pixel within a 31x31—and 91x91—pixel frame and permits groups of pixels to be assessed at a neighborhood level (Myint 2010). Accordingly, this enlarges the fundamental unit of analysis from just one pixel to several, allowing an improved assessment of the areas surrounding each pixel, minimizing inherent locational errors in the imagery. Finally, the latter two outputs were degraded to scaling factors 30x30—and 90x90—meters respectively, creating two images, the pixel values of which now represented percent-cover (see Figure 3.4).


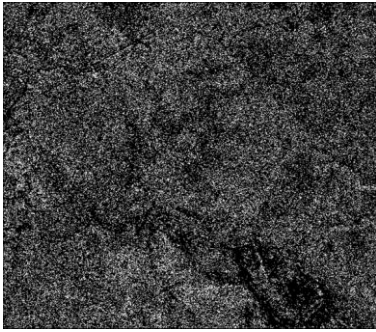

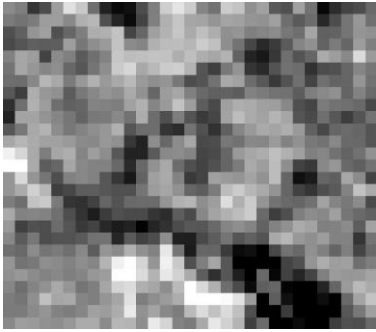
NAIP Orthophoto Transformations	
Transformation	Output
NAIP	
Recoded NAIP	
Degraded NAIP - 30m	
Degraded NAIP - 90m	

Figure 3.4 Orthophoto transformations. The original orthorectified NAIP (top) was recoded into 2 classes (forest and non-forest) through an unsupervised classification. The resulting recode was degraded to 30 m and 90 m resolutions to reduce locational error, making the aerial and satellite imagery more comparable.

3.3.2 Band Transformations

A total of six spectral enhancement algorithms, Principal Component Analysis (PCA), Tasseled Cap Transformation (TCT), Normalized Differentiation Vegetation Index (NDVI), Enhanced Vegetation Index (EVI), Simple Ratio Vegetation Index (RVI), and Soil-Adjusted Vegetation Index (SAVI), were used to optimize the *spectral* data (see Table 3.3). By mathematically merging the values of various bands, certain redundant bands of data were condensed, decreasing signature confusion. This method permitted the extraction of new, more interpretable bands (or layers) of data, making certain features, such as canopy cover, more distinguishable.

Table 3.3 Landsat-5 TM band transformation algorithms used in this study.

Index	Equation	Utility	Source
PCA (Principal Component Analysis)	See Lillesand and Kiefer 1972	Simplifies, compresses, reduces data overlap/redundancy	Lillesand and Kiefer 1972
TCT (Tasseled Cap Transformation)	$-0.273 b_1 - 0.217 b_2 - 0.551 b_3 + 0.722 b_4 + 0.073 b_5 - 0.165 b_7$	Simplifies, compresses, reduces data overlap/redundancy	Kauth and Thomas 1976, Crist and Cicone 1984
NDVI (Normalized Difference VI ^a)	$(NIR^b - Red) / (NIR + Red)$	Accentuates green biomass and LAI ^c	Kriegler et al. 1969, Rouse et al. 1973
EVI (Enhanced VI)	$2.5 ((NIR - Red) / (NIR + Red + L^d))$	Filters atmospheric and soil noise	Liu and Huete 1995
RVI (Simple Ratio VI)	NIR / Red	Segregates green vegetation and bare soil	Jordan 1969
SAVI (Soil-Adjusted VI)	$((NIR - Red) (1 + 0.5)) / (NIR + Red + L)$	Minimizes effect of soil background conditions	Huete 1988

^a Vegetation Index; ^b Near-infrared; ^c Leaf area index; ^d 0.5, dependent on LAI, but 0.5 reduces soil noise if applied to heterogeneous range of LAI values (Huete 1988).

Three local windows (3x3, 5x5, 7x7) were used to address the *spatial* arrangement and local variability of pixels within the study area. This operated much like the speckle suppression filters discussed previously (in section 3.3.1), except on the effect of a smaller scale (3x3, 5x5, and 7x7 pixels rather than 31x31 and 91x91).

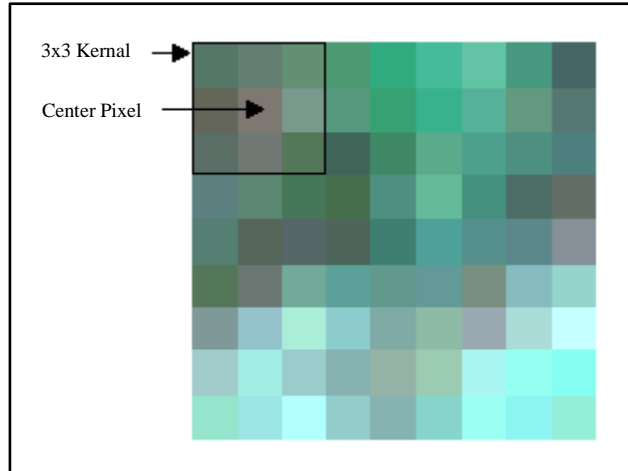


Figure 3.5 Example of a 3x3 local window used to decrease locational error by averaging pixel values at a neighborhood-level, which assigns a new value to each center pixel as the window (or “kernel”) systematically shifts across the imagery.

Finally, the transformed outputs were stacked as layers and combined into one file to extract the digital values of each pixel of interest (i.e., those that intersected a plot), thereby preparing the data for three sets of preliminary multiple linear regression (MLR) analyses. The way in which the nine transformations were applied to the imagery, as well as the layering of the resulting outputs, are depicted in Figure 3.6. See Figure 3.7 for the final outputs used for the preliminary linear regression, which determined the coefficients used to construct each model.

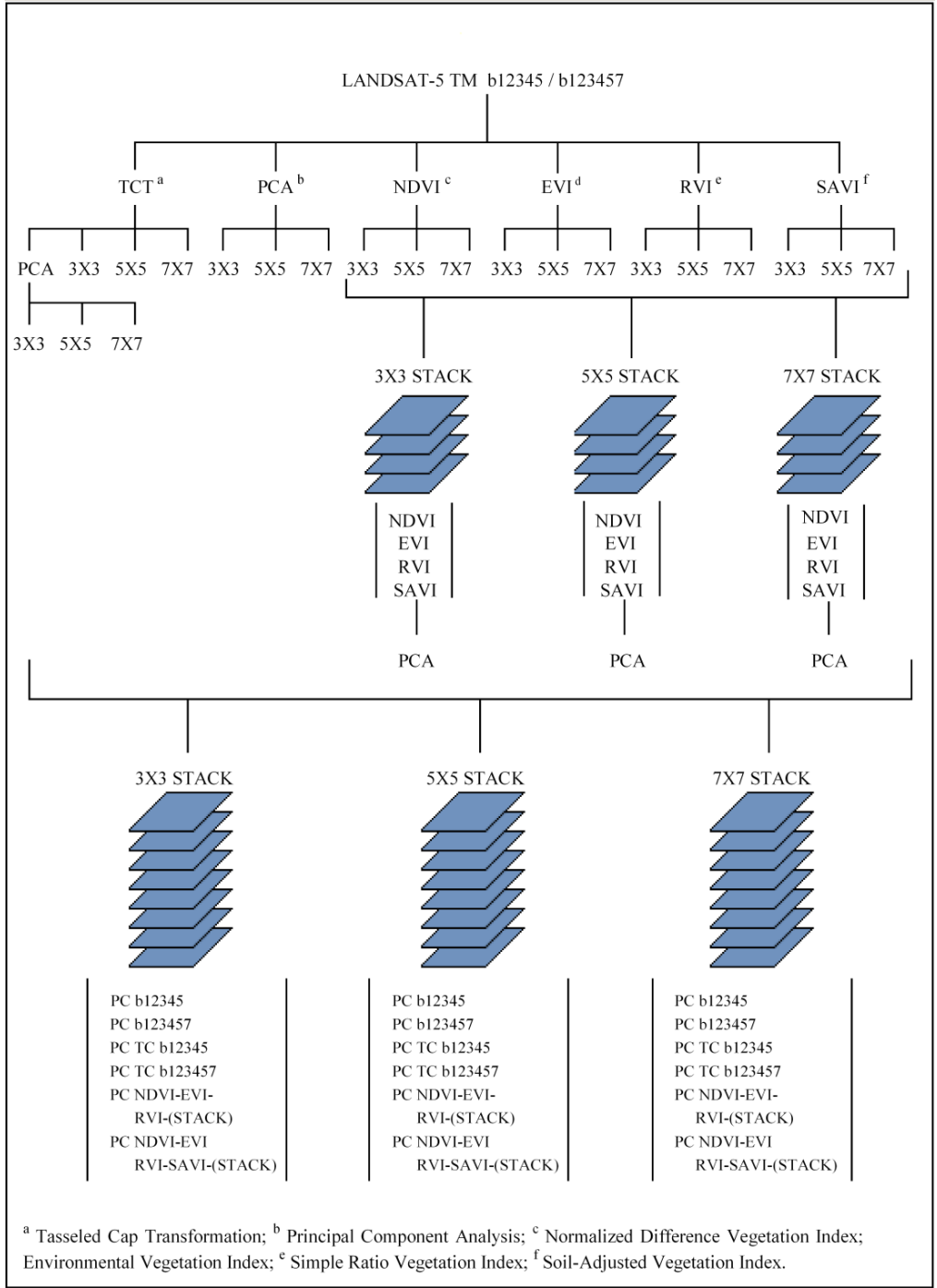


Figure 3.6 Band transformation decision-tree, which illustrates the transformations, their application to the imagery, and the layered outputs of the 9 transformations used for analysis.

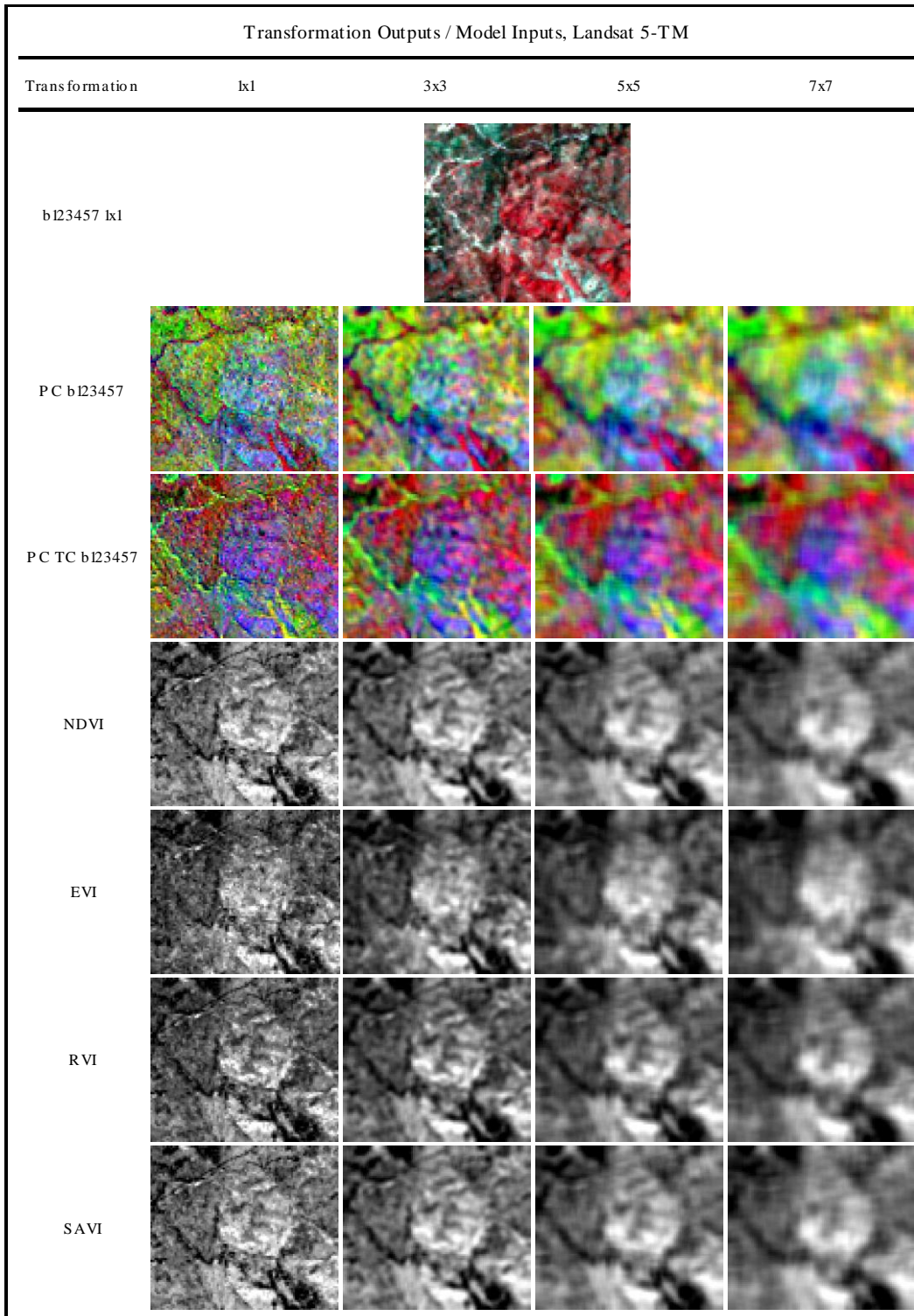


Figure 3.7 Transformation outputs and model inputs used for 3 sets (mixed, coniferous, and deciduous) of preliminary multiple linear regression analyses. The resulting coefficients were used to construct 54 models. Note: Imagery associated with b123457 1x1, PC b123457, and PC TC b123457 are 432 color composites. Black and white imagery associated with NDVI, EVI, RVI, SAVI signifies percent-cover; true black represents 0% while true white represents 100%.

3.3.3 Pre-Model Statistical Analyses

From the first set of 3x3, 5x5, and 7x7 layered stacks (i.e., the first set of stacks in Figure 3.6), the digital values of individual pixels (those that intersected the largest area of their respective plot) were used in a preliminary MLR analysis to test their relationship to the average percent-cover of the plot they represent. This procedure was followed for three different combinations of data. To measure the correlation between observed and modeled values across a mixture of coniferous and deciduous canopies, the first set of MLR analyses evaluated all plots (P1-P17, A1-A6, and K1-K7). The second set of MLR analyses evaluated the predictability of coniferous canopies (plots P1-P17), and the third set of MLR analyses evaluated deciduous plots (A1-A6 and K1-K7). Because no plot accounted for 0% canopy cover, as the boundary of each plot intercepted no less than two trees of interest (discussed in section 3.2.1), three additional pixels (with exceptionally low digital values; i.e., nearly 0% canopy cover) were added to each dataset in this part of the analysis as a frame of reference. Thus while 0% canopy cover was not expressed in the field data, by adding three additional pixels (or “pseudo-plots”) to the analysis, this reduced discontinuity and normalized the natural range of these data to provide the models with a baseline from which they could better identify patterns that are inherent to the landscape. The resulting intercept and regression coefficients for each transformation (or transformation-combination) provide the basis for 54 models (18 coniferous models, 18 deciduous models, and 18 mixed-cover models) that were designed to predict percent-cover across the entire study area.

3.3.4 Model Construction

In conjunction with the band values of the transformed outputs selected above, the intercept and regression coefficients produced by the pre-model regression analyses were used to construct 54 models: 18 mixed canopy models (to predict coniferous and deciduous canopy cover), 18 coniferous canopy models, and 18 deciduous canopy models (see equation below, as well as Tables 3.4, 3.5, and 3.6). The following equation uses the regression coefficients produced by the preliminary statistical analyses (from the first set of stacks in Figure 3.6) with the relative band value of each transformed output from each group of data (mixed, coniferous, deciduous). Thus, by fitting the pre-modeled band values to measured field data, pre-model regression metrics

produced the calibration coefficients (training data) used to generate a model that has been prepared to simulate canopy cover for the entire study area.

$$y = b + (m1 * B1) + (m2 * B2)...(mx * Bx)...$$

b = intercept coefficient

m = regression coefficient

B = variable (Landsat-5 TM band)

Table 3.4 Mixed coniferous and deciduous forest-cover model equations.

Mixed Cover		
Window	Transformation	Basic Equation
3x3	PC ^a B12345	163.166 - (0.275 *B1)+(0.091*B2)-(0.080 *B3)- (0.403 *B4)- (0.360 *B5)
	PC B123457	176.626 - (0.264 *B1)+(0.087 *B2)-(0.085 *B3)- (0.396 *B4)- (0.378 *B5)- (0.095 *B7)
	PC TC ^b B12345	143.595 - (0.272 *B1)+(0.088 *B2)+(0.080 *B3)- (0.405 *B4)- (0.365 *B5)
	PC TC B123457	131928 - (0.263 *B1)+(0.084 *B2)+(0.084 *B3)- (0.397 *B4)- (0.382 *B5)+ (0.092 *B7)
	PC NDVI ^c -EVI ^d -RVI ^e (STACK)	15.268 + (0.254 *NDVI)- (0.041 *EVI)- (0.146 *RVI)
	PC NDVI-EVI-RVI-SAVI ^f (STACK)	1655 + (0.244 *NDVI)- (0.034 *EVI)- (0.144 *RVI)+ (0.093 *SAVI)
5x5	PC B12345	145.175 - (0.340 *B1)+(0.117 *B2)+(0.071*B3)- (0.347 *B4)- (0.470 *B5)
	PC B123457	125.952 - (0.338 *B1)+(0.126 *B2)+(0.082 *B3)- (0.367 *B4)- (0.446 *B5)+ (0.130 *B7)
	PC TC B12345	165.164 - (0.339 *B1)+(0.115 *B2)- (0.069 *B3)- (0.359 *B4)- (0.474 *B5)
	PC TC B123457	182.504 - (0.337 *B1)+(0.124 *B2)- (0.080 *B3)- (0.380 *B4)- (0.449 *B5)- (0.134 *B7)
	PC NDVI-EVI-RVI (STACK)	14.125 + (0.308 *NDVI)- (0.056 *EVI)- (0.265 *RVI)
	PC NDVI-EVI-RVI-SAVI (STACK)	-14.360 + (0.299 *NDVI)- (0.066 *EVI)- (0.274 *RVI)+ (0.207 *SAVI)
7x7	PC B12345	130.708 - (0.399 *B1)+(0.143 *B2)+(0.188 *B3)- (0.306 *B4)- (0.552 *B5)
	PC B123457	136.35 - (0.398 *B1)+(0.141 *B2)+(0.182 *B3)- (0.302 *B4)- (0.554 *B5)- (0.040 *B7)
	PC TC B12345	180.702 - (0.400 *B1)+(0.142 *B2)- (0.183 *B3)- (0.316 *B4)- (0.561 *B5)
	PC TC B123457	172.631 - (0.399 *B1)+(0.139 *B2)- (0.176 *B3)- (0.309 *B4)- (0.565 *B5)+ (0.055 *B7)
	PC NDVI-EVI-RVI (STACK)	14.690 + (0.371 *NDVI)- (0.108 *EVI)- (0.280 *RVI)
	PC NDVI-EVI-RVI-SAVI (STACK)	-34.075 + (0.359 *NDVI)- (0.143 *EVI)- (0.342 *RVI)+ (0.373 *SAVI)

^a Principal Components; ^b Tasseled Components; ^c Normalized Difference Vegetation Index; ^d Environmental Vegetation Index; ^e Simple Ratio Vegetation Index; ^f Soil-Adjusted Vegetation Index.

Table 3.5 Coniferous forest-cover model equations.

Coniferous Cover		
Window	Transformation	Basic Equation
3x3	PC ^a B12345	132.770 - (0.253 *B1)+ (0.114 *B2)- (0.008 *B3)- (0.306 *B4)- (0.355 *B5)
	PC B123457	127.974 - (0.255 *B1)+ (0.112 *B2)- (0.003 *B3)- (0.305 *B4)- (0.348 *B5)+ (0.025 *B7)
	PC TC ^b B12345	130.377 - (0.246 *B1)+ (0.111 *B2)- (0.002 *B3)- (0.299 *B4)- (0.358 *B5)
	PC TC B123457	133.587 - (0.248 *B1)+ (0.108 *B2)- (0.007 *B3)- (0.298 *B4)- (0.350 *B5)- (0.027 *B7)
	PC NDVI ^c -EVI ^d -RVI ^e (STACK)	24.409 + (0.307 *NDVI)- (0.171 *EVI)- (0.079 *RVI)
	PC NDVIEVIRVLSAVI ^f (STACK)	16.945 + (0.296 *NDVI)- (0.160 *EVI)- (0.084 *RVI)+ (0.052 *SAVI)
5x5	PC B12345	91902 - (0.351 *B1)+ (0.096 *B2)+ (0.164 *B3)- (0.063 *B4)- (0.471 *B5)
	PC B123457	27.427 - (0.326 *B1)+ (0.098 *B2)+ (0.237 *B3)- (0.092 *B4)- (0.381 *B5)+ (0.339 *B7)
	PC TC B12345	139.465 - (0.350 *B1)+ (0.092 *B2)- (0.159 *B3)- (0.089 *B4)- (0.488 *B5)
	PC TC B123457	183.025 - (0.322 *B1)+ (0.093 *B2)- (0.237 *B3)- (0.123 *B4)- (0.398 *B5)- (0.354 *B7)
	PC NDVIEVIRVI (STACK)	34.173 + (0.382 *NDVI)- (0.309 *EVI)- (0.118 *RVI)
	PC NDVIEVIRVLSAVI (STACK)	3.299 + (0.340 *NDVI)- (0.309 *EVI)- (0.163 *RVI)+ (0.245 *SAVI)
7x7	PC B12345	103.577 - (0.467 *B1)+ (0.109 *B2)+ (0.199 *B3)- (0.106 *B4)- (0.503 *B5)
	PC B123457	84.462 - (0.461 *B1)+ (0.110 *B2)+ (0.233 *B3)- (0.116 *B4)- (0.503 *B5)+ (0.113 *B7)
	PC TC B12345	161.579 - (0.466 *B1)+ (0.107 *B2)- (0.203 *B3)- (0.132 *B4)- (0.528 *B5)
	PC TC B123457	178.704 - (0.461 *B1)+ (0.108 *B2)- (0.234 *B3)- (0.142 *B4)- (0.527 *B5)- (0.106 *B7)
	PC NDVIEVIRVI (STACK)	34.835 + (0.463 *NDVI)- (0.375 *EVI)- (0.135 *RVI)
	PC NDVIEVIRVLSAVI (STACK)	-1986 + (0.410 *NDVI)- (0.360 *EVI)- (0.239 *RVI)+ (0.288 *SAVI)

^a Principal Components; ^b Tasseled Components; ^c Normalized Difference Vegetation Index; ^d Environmental Vegetation Index; ^e Simple Ratio Vegetation Index; ^f Soil-Adjusted Vegetation Index.

Table 3.6 Deciduous forest-cover model equations.

Deciduous Cover		
Window	Transformation	Basic Equation
3x3	PC ^a B12345	147.257 - (0.235 *B1)+(0.112 *B2)-(0.050 *B3)-(0.444 *B4)- (0.294 *B5)
	PC B123457	183.191 - (0.196 *B1)+(0.065 *B2)-(0.047 *B3)-(0.402 *B4)- (0.344 *B5)- (0.280 *B7)
	PC TC ^b B12345	137.148 - (0.241*B1)+(0.105 *B2)+(0.058 *B3)-(0.456 *B4)- (0.296 *B5)
	PC TC B123457	104.035 - (0.205 *B1)+(0.058 *B2)+(0.054 *B3)-(0.415 *B4)- (0.341*B5)+(0.267 *B7)
	PC NDVI ^c -EVI ^d -RVI ^e (STACK)	-8.917 + (0.236 *NDVI) + (0.145 *EVI) - (0.151 *RVI)
	PC NDVI-EVI-RVI-SAVI ^f (STACK)	-172.750 + (0.285 *NDVI) + (0.551 *EVI) + (0.108 *RVI) + (0.642 *SAVI)
5x5	PC B12345	38.282 - (0.0136 *B1)+(0.424 *B2)+(0.175 *B3)-(0.277 *B4)- (0.403 *B5)
	PC B123457	36.372 - (0.025 *B1)+(0.422 *B2)+(0.173 *B3)- (0.304 *B4)- (0.400 *B5)+(0.059 *B7)
	PC TC B12345	71.725 + (0.015 *B1)+(0.449 *B2)- (0.179 *B3)- (0.250 *B4)- (0.391*B5)
	PC TC B123457	84.012 + (0.005 *B1)+(0.447 *B2)- (0.177 *B3)- (0.276 *B4)- (0.388 *B5)- (0.058 *B7)
	PC NDVI-EVI-RVI (STACK)	-17.431 + (0.292 *NDVI) + (0.191 *EVI) - (0.288 *RVI)
	PC NDVI-EVI-RVI-SAVI (STACK)	-151.425 + (0.348 *NDVI) + (0.441 *EVI) - (0.071 *RVI) + (0.597 *SAVI)
7x7	PC B12345	-88.119 + (0.141*B1)+(0.593 *B2)+(0.416 *B3)- (0.040 *B4)- (0.287 *B5)
	PC B123457	-86.379 + (0.187 *B1)+(0.614 *B2)+(0.405 *B3)+(0.056 *B4)- (0.271*B5)- (0.183 *B7)
	PC TC B12345	-3.445 + (0.181*B1)+(0.632 *B2)- (0.419 *B3)+(0.022 *B4)- (0.255 *B5)
	PC TC B123457	-63.078 + (0.240 *B1)+(0.659 *B2)- (0.405 *B3)+(0.142 *B4)- (0.237 *B5)+(0.231*B7)
	PC NDVI-EVI-RVI (STACK)	-28.274 + (0.356 *NDVI) + (0.232 *EVI) - (0.311 *RVI)
	PC NDVI-EVI-RVI-SAVI (STACK)	-118.314 + (0.386 *NDVI) + (0.317 *EVI) - (0.224 *RVI) + (0.491 *SAVI)

^a Principal Components; ^b Tasseled Components; ^c Normalized Difference Vegetation Index; ^d Environmental Vegetation Index; ^e Simple Ratio Vegetation Index; ^f Soil-Adjusted Vegetation Index.

3.3.5 Predicting Canopy Cover

The 54 models were applied to the Landsat image to predict percent-cover on a pixel-by-pixel basis for the entire study area. This entailed a computer-automated recognition of statistical patterns defined by the transformations above. Through this, additional layers are derived through the extraction of spectral—(NDVI, EVI, RVI, SAVI) and textural—(PCA and TCT) patterns.

3.3.6 Model Accuracy

The accuracy of these models is tested against a 2007 classified (unsupervised) orthophoto (degraded from 1 m to 30 and 90 m resolutions, producing two different outputs). Final linear regression analyses compare 100 random pixels from the modeled outputs to both classified orthophotos (with 30m and 90m resolutions), and calculate the significance of each model's ability to predict percent-cover. All of the above was done in three steps, discussed below.

First, the pixel values of 100 pixels were selected at random from a 55-layer stack of 54 model-outputs associated with a classified 30-meter degraded NAIP orthophoto. By selecting 100 pixels from a stack of layered imagery, each of the 100 pixels could remain locationally congruent throughout each layer. Thus, when the digital value of a random pixel has been extracted from layer one, the digital value of the same random pixel would be extracted from layers 1-55. Therefore, each selected pixel was an expression of the same or similar land features—percent-cover. These steps were repeated by replacing the 30-meter orthophoto with the 90-meter orthophoto. Next, a quick correlation showed which of the 54 transformations predicted percent-cover most accurately. Finally, those transformations with the most positively-correlated pixel values for percent-cover were examined more closely and a post-model MLR analysis was used to learn more about the relationship between observed and predicted values of percent-cover.

CHAPTER 4

RESULTS

4.1 Pre-Model Statistical Analyses

The correlation between observed and modeled values (i.e., the relationship between *in situ* mixed, coniferous, and deciduous percent-cover averages and the transformed digital value of each respective pixel) for those pixels that intersected the largest area of their respective plot was tested through three sets of preliminary multiple linear regression analyses (MLR) (see Tables 4.1, 4.2 and 4.3). In general, as local window size increased, the coefficients of determination (or, the percentage of shared variance between values derived by observed and modeled canopy cover totals based on intersecting plot-pixels) for mixed and coniferous cover decreased. In addition, regardless of cover-type (mixed, coniferous, deciduous) or local window resolution (3x3, 5x5, 7x7), the principal and tasseled cap components of all multispectral bands (bands 123457) outperformed every other transformation across the board (in terms of r^2). Trailing closely behind were the principal and tasseled cap components of bands 12345 and the principal components of bands 123457.

Table 4.1 Results of pre-model multiple linear regression analyses for mixed forest canopy cover based on 33 observations (33-plot data).

Mixed Cover				
Local Window	Transformation	Multiple R	R ²	Standard Error
3x3	PC ^a b12345	0.853	0.727	8.587
	PC b123457	0.855	0.732	8.683
	PC TC ^b b12345	0.855	0.731	8.527
	PC TC b123457	0.857	0.735	8.627
	PC NDVI ^c -EVI ^d -RVI ^e (stack)	0.777	0.604	9.982
	PC NDVI-EVI-RVI-SAVI ^f (stack)	0.783	0.613	10.048
5x5	PC b12345	0.803	0.644	9.808
	PC b123457	0.805	0.648	9.950
	PC TC b12345	0.804	0.647	9.779
	PC TC b123457	0.806	0.650	9.916
	PC NDVI-EVI-RVI (stack)	0.762	0.581	10.275
	PC NDVI-EVI-RVI-SAVI (stack)	0.778	0.605	10.153
7x7	PC b12345	0.799	0.639	9.881
	PC b123457	0.800	0.639	10.066
	PC TC b12345	0.801	0.641	9.852
	PC TC b123457	0.801	0.642	10.034
	PC NDVI-EVI-RVI (stack)	0.746	0.557	10.565
	PC NDVI-EVI-RVI-SAVI (stack)	0.788	0.622	9.935

^a Principal Components; ^b Tasseled Components; ^c Normalized Difference Vegetation Index; ^d Environmental Vegetation Index; ^e Simple Ratio Vegetation Index; ^f Soil-Adjusted Vegetation Index

Table 4.2 Results of pre-model multiple linear regression analyses for coniferous forest canopy cover based on 16 observations (16-plot data).

Coniferous Cover				
Local Window	Transformation	Multiple R	R ²	Standard Error
3x3	PC ^a b12345	0.874	0.764	9.543
	PC b123457	0.874	0.764	9.900
	PC TC ^b b12345	0.875	0.765	9.510
	PC TC b123457	0.875	0.765	9.865
	PC NDVI ^c -EVI ^d -RVI ^e (stack)	0.873	0.763	8.940
	PC NDVI-EVI-RVI-SAVI ^f (stack)	0.875	0.765	9.190
5x5	PC b12345	0.868	0.753	9.763
	PC b123457	0.873	0.762	9.945
	PC TC b12345	0.868	0.753	9.752
	PC TC b123457	0.874	0.763	9.916
	PC NDVI-EVI-RVI (stack)	0.856	0.733	9.479
	PC NDVI-EVI-RVI-SAVI (stack)	0.871	0.759	9.309
7x7	PC b12345	0.869	0.755	9.726
	PC b123457	0.869	0.755	10.077
	PC TC b12345	0.870	0.758	9.664
	PC TC b123457	0.871	0.758	10.015
	PC NDVI-EVI-RVI (stack)	0.855	0.730	9.536
	PC NDVI-EVI-RVI-SAVI (stack)	0.873	0.762	9.247

^a Principal Components; ^b Tasseled Components; ^c Normalized Difference Vegetation Index; ^d Environmental Vegetation Index; ^e Simple Ratio Vegetation Index; ^f Soil-Adjusted Vegetation Index

Table 4.3 Results of pre-model multiple linear regression analyses for deciduous forest canopy cover based on 20 observations (20-plot data).

Deciduous Cover				
Local Window	Transformation	Multiple R	R ²	Standard Error
3x3	PC ^a b12345	0.924	0.853	7.854
	PC b123457	0.939	0.881	7.451
	PC TC ^b b12345	0.927	0.860	7.675
	PC TC b123457	0.941	0.885	7.323
	PC NDVI ^c -EVI ^d -RVI ^e (stack)	0.850	0.723	9.846
	PC NDVI-EVI-RVI-SAVI ^f (stack)	0.929	0.863	7.227
5x5	PC b12345	0.904	0.816	8.782
	PC b123457	0.904	0.817	9.238
	PC TC b12345	0.904	0.818	8.745
	PC TC b123457	0.905	0.819	9.200
	PC NDVI-EVI-RVI (stack)	0.866	0.749	9.365
	PC NDVI-EVI-RVI-SAVI (stack)	0.923	0.851	7.536
7x7	PC b12345	0.925	0.856	7.771
	PC b123457	0.928	0.861	8.053
	PC TC b12345	0.928	0.861	7.639
	PC TC b123457	0.932	0.869	7.832
	PC NDVI-EVI-RVI (stack)	0.872	0.760	9.160
	PC NDVI-EVI-RVI-SAVI (stack)	0.921	0.848	7.624

^a Principal Components; ^b Tasseled Components; ^c Normalized Difference Vegetation Index; ^d Environmental Vegetation Index; ^e Simple Ratio Vegetation Index; ^f Soil-Adjusted Vegetation Index

4.2 Post-Model Statistical Analyses

4.2.1 Correlation and Post-Model Multiple Linear Regression Analysis

Based on the 100 random pixels selected from the 55-layer stack (made up of the 54 transformations and 1 classified NAIP orthophoto), the post-model correlation showed which of the 54 transformations predicted percent-cover most accurately when compared to the 30- and 90-meter classified NAIP orthophotos. To permit a closer examination of the transformations that yielded pixel values (percent-cover totals) most similar to those observed in the field, those transformations with more negatively-correlated pixel values (i.e., dissimilar percent-cover totals) were removed from all further analyses (see all model outputs, the layers from which 100 pixels were sampled, in Figures 4.1, 4.2, and 4.3).

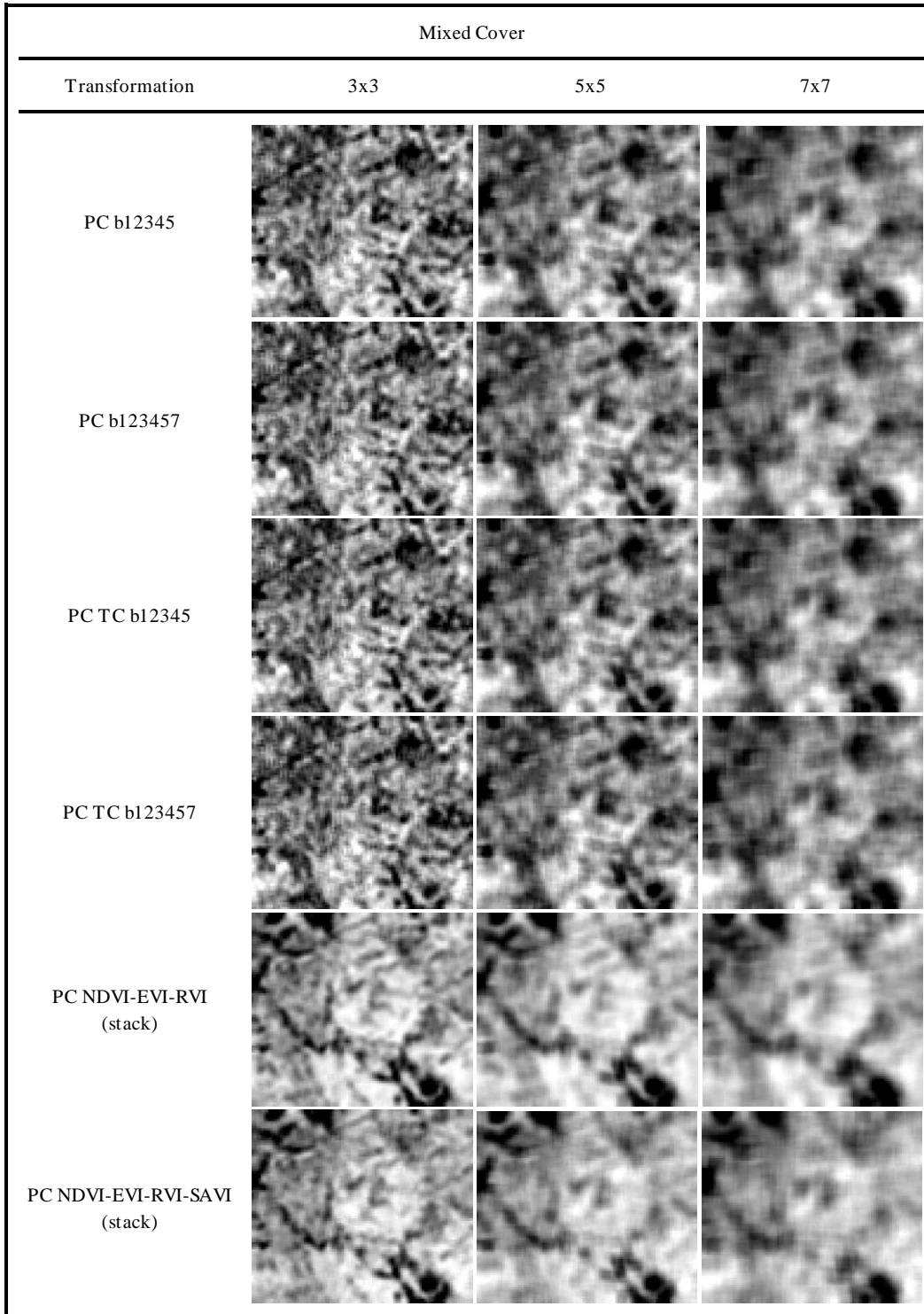


Figure 4.1 Percent-cover model outputs for mixed forest cover plots. Black to white gradient has been scaled to signify percent-cover; true black represents 0% cover while true white represents 100% cover.

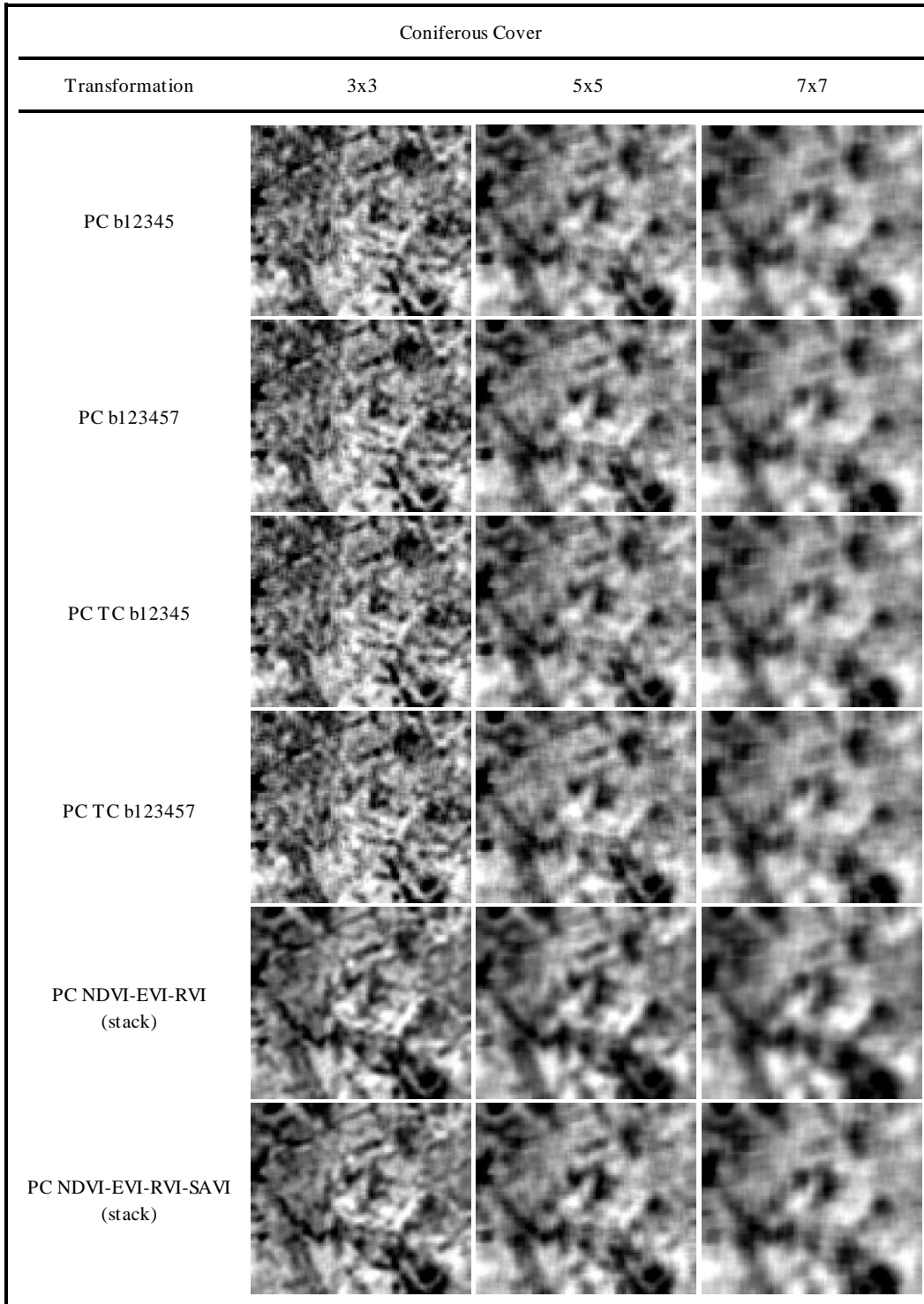


Figure 4.2 Percent-cover model outputs for coniferous forest cover. Black to white gradient has been scaled to signify percent-cover; true black represents 0% cover while true white represents 100% cover.

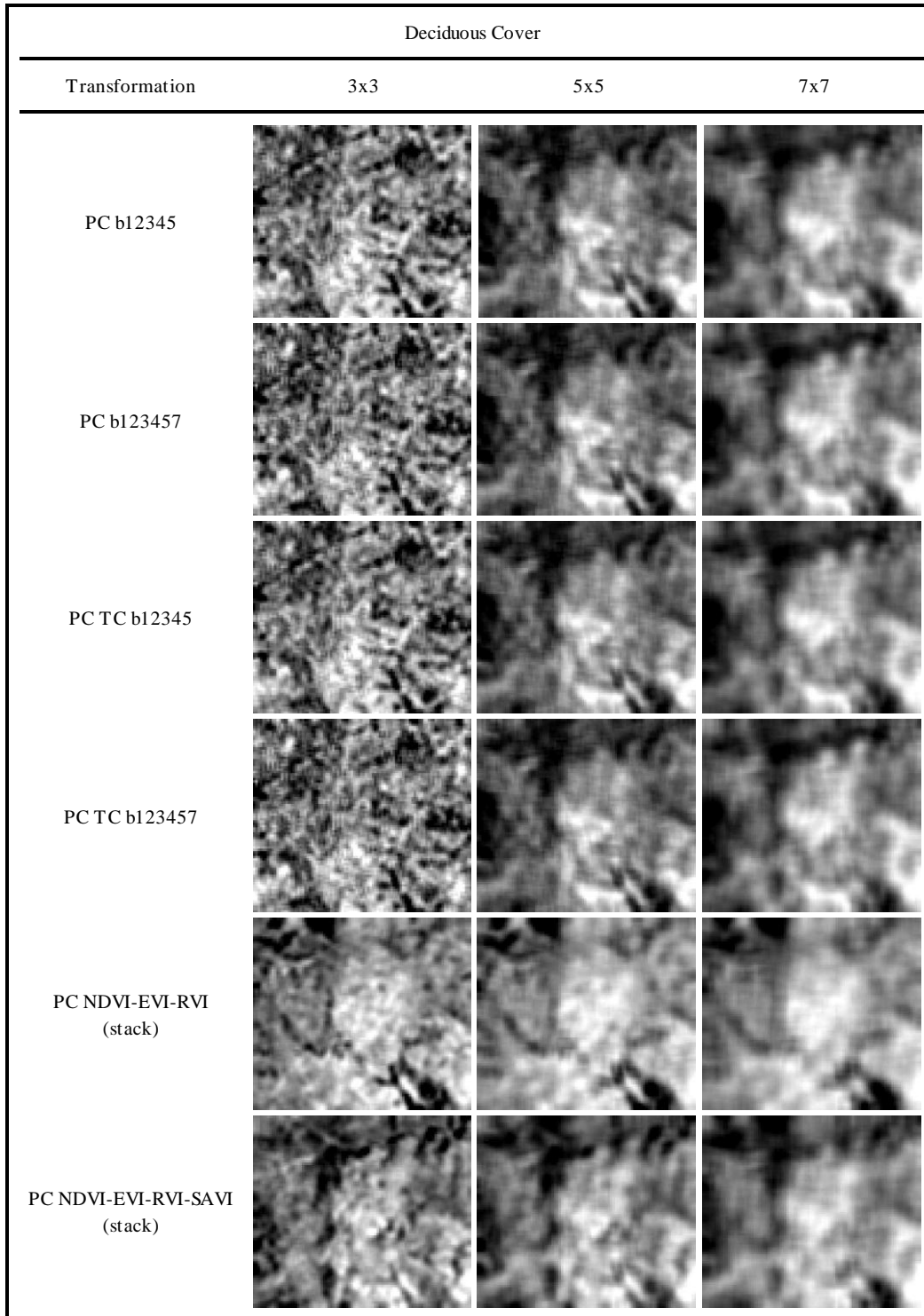


Figure 4.3 Percent-cover model outputs for deciduous forest cover. Black to white gradient has been scaled to signify percent-cover; true black represents 0% cover while true white represents 100% cover.

Table 4.4 reveals that regardless of cover-type (mixed, coniferous, deciduous) or local window size (3x3, 5x5, 7x7), the principal components of three vegetation indices (NDVI-EVI-RVI) were correlated more positively than any other transformation. The 3x3 principal component transformations of all four vegetation indices (NDVI-EVI-RVI-SAVI) are also noteworthy. Eleven models were selected for further analysis by applying a threshold of value of 0.80 to the post-model correlation coefficients (see bold-faced values in Table 4.4). Figures 4.4 and 4.5 illustrate the post-model (as opposed to preliminary) MLR results for the eleven models chosen for further analyses. Tables 4.5 and 4.6 display the MLR results in table format, as well as the significance of the models.

Table 4.4 Post-model correlation coefficients. Bold-faced values indicate the coefficients for the transformations chosen for final post-model analysis.

Cover	Landsat Transformation	Correlation Coefficient (r)					
		NAIP 30 meter			NAIP 90 meter		
		3x3	5x5	7x7	3x3	5x5	7x7
Mixed	PC ^a b12345	0.5781	0.6460	0.6641	0.5722	0.6825	0.6764
	PC b123457	0.5716	0.6427	0.6588	0.5691	0.6759	0.6728
	PC TC ^b b12345	0.5529	0.6579	0.6614	0.5467	0.6967	0.6733
	PC TC b123457	0.5476	0.6546	0.6548	0.5447	0.6900	0.6682
	PC NDVI ^c -EVI ^d -RVI ^e (stack)	0.8514	0.7907	0.7537	0.8677	0.8369	0.7806
	PC NDVI-EVI-RVI-SAVI ^f (stack)	0.8156	0.7160	0.6332	0.8346	0.77935	0.6590
Coniferous	PC b12345	0.6588	0.7109	0.6988	0.6765	0.7344	0.7091
	PC b123457	0.6586	0.7008	0.6916	0.6812	0.7260	0.7028
	PC TC b12345	0.6654	0.7436	0.7042	0.6836	0.7606	0.7123
	PC TC b123457	0.6654	0.7326	0.6969	0.6885	0.7502	0.7060
	PC NDVI-EVI-RVI (stack)	0.8627	0.8157	0.7645	0.8602	0.8156	0.7762
	PC NDVI-EVI-RVI-SAVI (stack)	0.8586	0.7586	0.7082	0.8579	0.76843	0.7283
Deciduous	PC b12345	0.5789	0.4784	0.4399	0.5607	0.3692	0.1380
	PC b123457	0.5680	0.4635	0.4264	0.5521	0.3272	0.1147
	PC TC b12345	0.4500	0.4851	0.4185	0.4303	0.3859	0.1078
	PC TC b123457	0.4482	0.4700	0.3993	0.4336	0.3422	0.0799
	PC NDVI-EVI-RVI (stack)	0.6362	0.5740	0.5409	0.6735	0.6284	0.5470
	PC NDVI-EVI-RVI-SAVI (stack)	0.1240	0.2597	0.3733	-0.1352	0.0573	0.2241

^a Principal Components; ^b Tasseled Components; ^c Normalized Difference Vegetation Index; ^d Environmental Vegetation Index; ^e Simple Ratio Vegetation Index; ^f Soil-Adjusted Vegetation Index

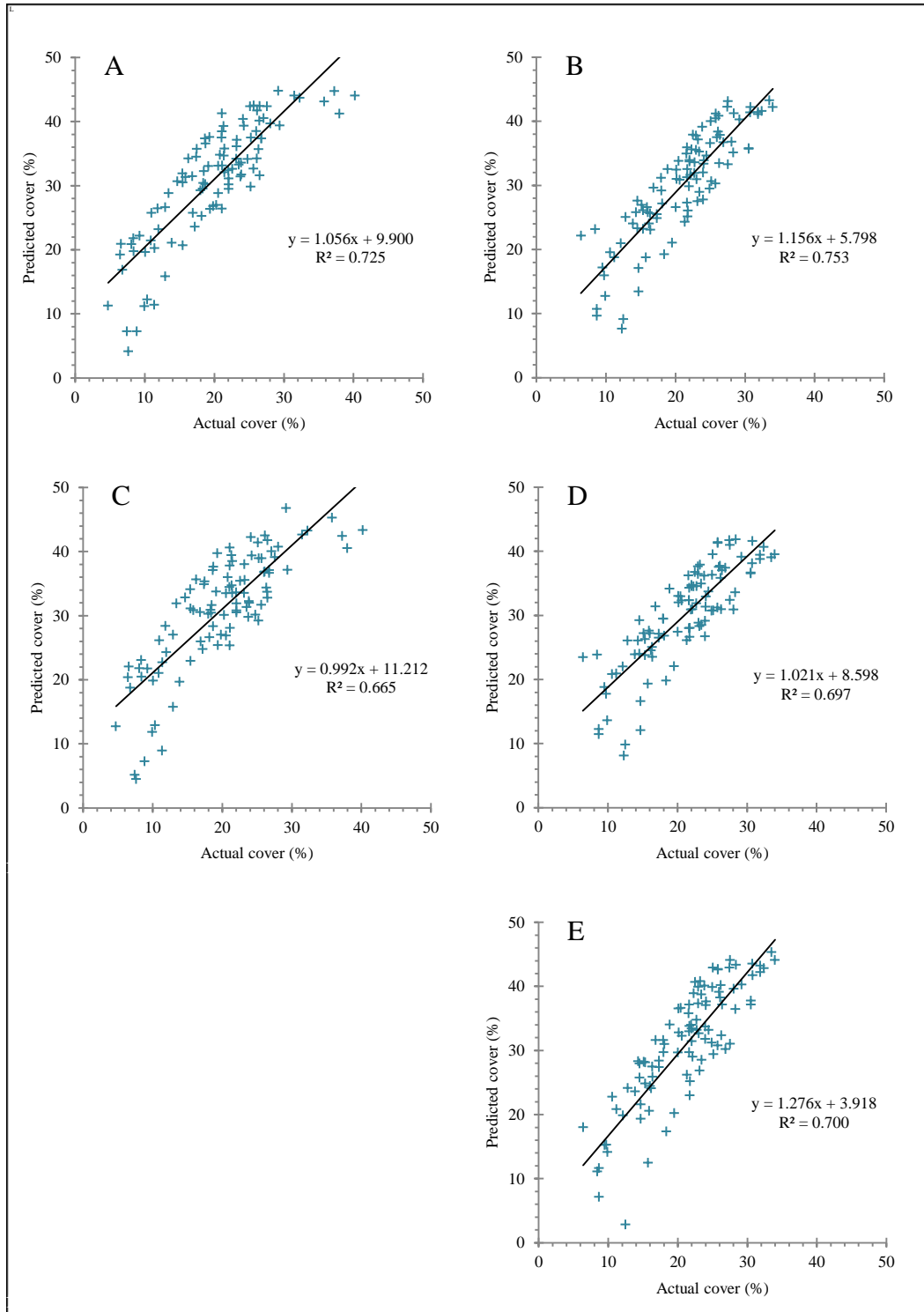


Figure 4.4 Post-model multiple linear regression vegetation fractions for mixed-cover by PC bands NDVI-EVI-RVI using: (A) 3x3 window and 30 m NAIP; (B) 3x3 window and 90 m NAIP; (E) 5x5 window and 90 m NAIP. Vegetation fractions by PC bands NDVI-EVI-RVI-SAVI using: (C) 3x3 window and 30 m NAIP; and (D) 3x3 window and 90 m NAIP.

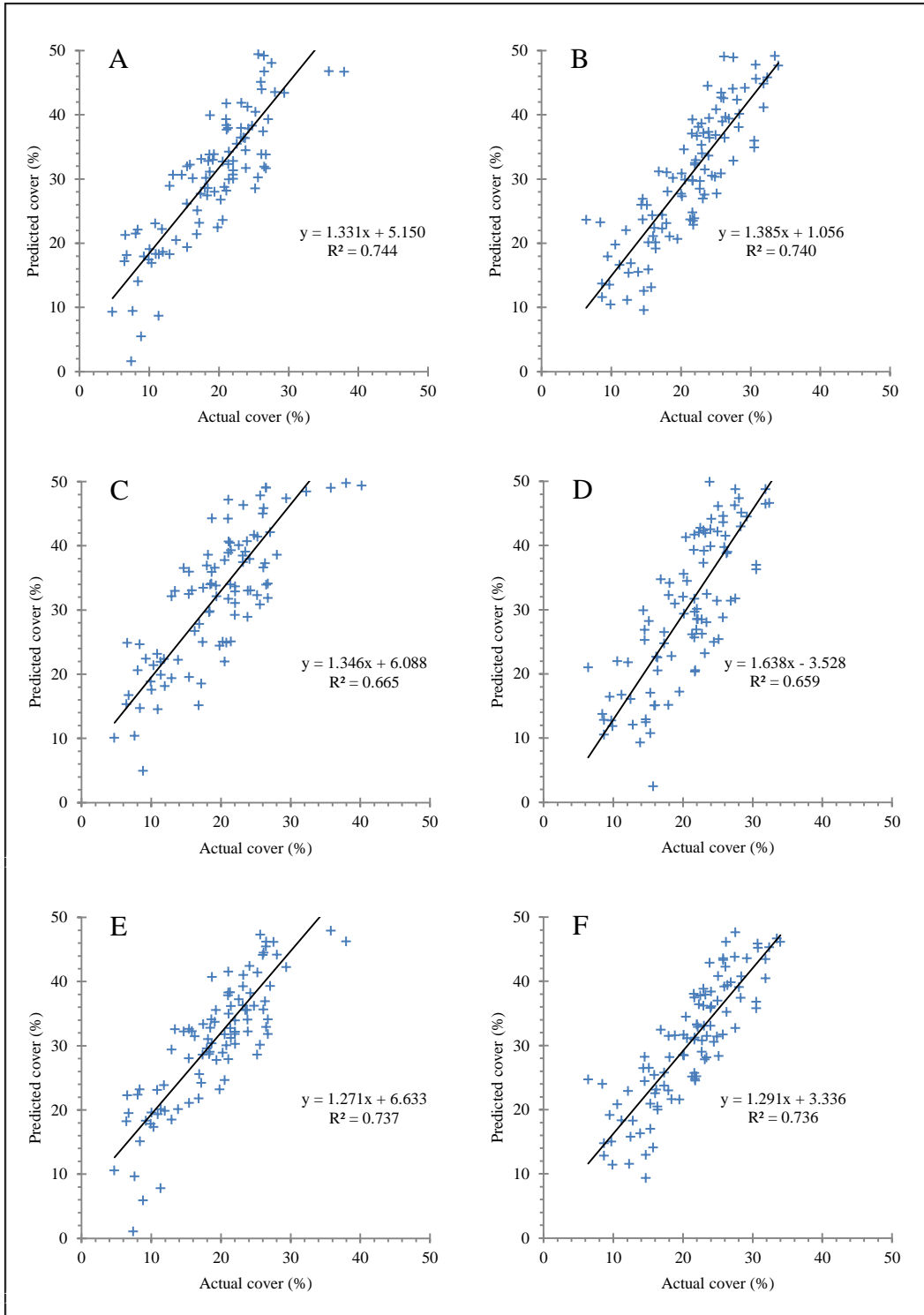


Figure 4.5 Post-model multiple linear regression vegetation fractions for coniferous-cover by PC bands NDVI-EVI-RVI using: (A) 3x3 window and 30 m NAIP; (B) 3x3 window and 90 m NAIP; (C) 30 m NAIP; and (D) 5x5 window and 90 m NAIP. Vegetation fractions by PC bands NDVI-EVI-RVI-SAVI using: (E) 3x3 window and 30 m NAIP; and (F) 3x3 window and 90 m NAIP.

Table 4.5 Post-model multiple linear regression results and p-value figures for final mixed forest canopy cover models.

Mixed Cover		
Transformation	Multiple R	R ²
PC ^a 3x3 NDVI ^b -EVI ^c -RVI ^d (stack)	0.851	0.725
	0.816	0.665
PC 5x5 NDVI-EVI-RVI (stack)	0.868	0.753
	0.837	0.700
PC 3x3 NDVI-EVI-RVI-SAVI ^e (stack)	0.835	0.697

^a Principal Components; ^b Normalized Difference Vegetation Index; ^c Environmental Vegetation Index; ^d Simple Ratio Vegetation Index; ^e Soil-Adjusted Vegetation Index. Note: All values are significant at the 0.01 level, i.e. $p < 0.01$

Table 4.6 Residual variance (bias) and root-mean-square error figures for final coniferous forest canopy cover models.

Coniferous Cover		
Transformation	Multiple R	R ²
PC ^a 3x3 NDVI ^b -EVI ^c -RVI ^d (stack)	0.863	0.744
	0.816	0.665
PC 5x5 NDVI-EVI-RVI (stack)	0.859	0.737
	0.860	0.740
PC 3x3 NDVI-EVI-RVI-SAVI ^e (stack)	0.812	0.659
	0.858	0.736

^a Principal Components; ^b Normalized Difference Vegetation Index; ^c Environmental Vegetation Index; ^d Simple Ratio Vegetation Index; ^e Soil-Adjusted Vegetation Index. Note: All values are significant at the 0.01 level, i.e. $p < 0.01$

4.2.2 Residual Variance

The residual variance figures (i.e., average deviation of predicted from observed values) indicate that modeled canopy cover estimates generally exceeded observed cover, over predicting percent-cover by a margin of about 9.0-12.9%; approximately 9.1-11.1% for mixed forest canopy cover and 9.1-12.9% for coniferous forest canopy cover (see Tables 4.5 and 4.6 and Figures 4.6 and 4.7). In terms of r^2 , the performance of models defined by the principal components of three

vegetation indices (NDVI, EVI, RVI) were superior (i.e., predicted percent-cover more accurately) to those defined by the principal components of all four (NDVI, EVI, RVI, SAVI). Models treated with three vegetation indices (NDVI, EVI, RVI) and a 3x3 local window predicted percent-cover more accurately than those treated with a 5x5 local window. These models predicted canopy cover most accurately when tested against the 90 meter orthophoto, regardless of cover-type or window resolution, indicating that the 30 meter orthophoto contained less locational accuracy.

Table 4.7 Residual variance (bias) and root-mean-square error figures for final mixed forest canopy cover models.

Mixed Cover			
Transformation	NAIP Res.	Bias	RMSE
PC ^a 3x3 NDVI ^b -EVI ^c -RVI ^d (stack)	30m	-11.012	12.141
	90m	-9.077	10.139
PC 5x5 NDVI-EVI-RVI (stack)	90m	-9.725	11.305
PC 3x3 NDVI-EVI-RVI-SAVI ^e (stack)	30m	-11.053	12.335
	90m	-9.029	10.078

^a Principal Components; ^b Normalized Difference Vegetation Index;
^c Environmental Vegetation Index; ^d Simple Ratio Vegetation Index;
^e Soil-Adjusted Vegetation Index.

Table 4.8 Residual variance (bias) and root-mean-square error figures for final coniferous forest canopy cover models.

Coniferous Cover			
Transformation	NAIP Res.	Bias	RMSE
PC ^a 3x3 NDVI ^b -EVI ^c -RVI ^d (stack)	30m	-11.695	13.393
	90m	-9.137	10.884
PC 5x5 NDVI-EVI-RVI (stack)	30m	-12.931	15.092
	90m	-9.879	13.125
PC 3x3 NDVI-EVI-RVI-SAVI ^e (stack)	30m	11.996	13.523
	90m	-9.450	10.898

^a Principal Components; ^b Normalized Difference Vegetation Index;
^c Environmental Vegetation Index; ^d Simple Ratio Vegetation Index;
^e Soil-Adjusted Vegetation Index.

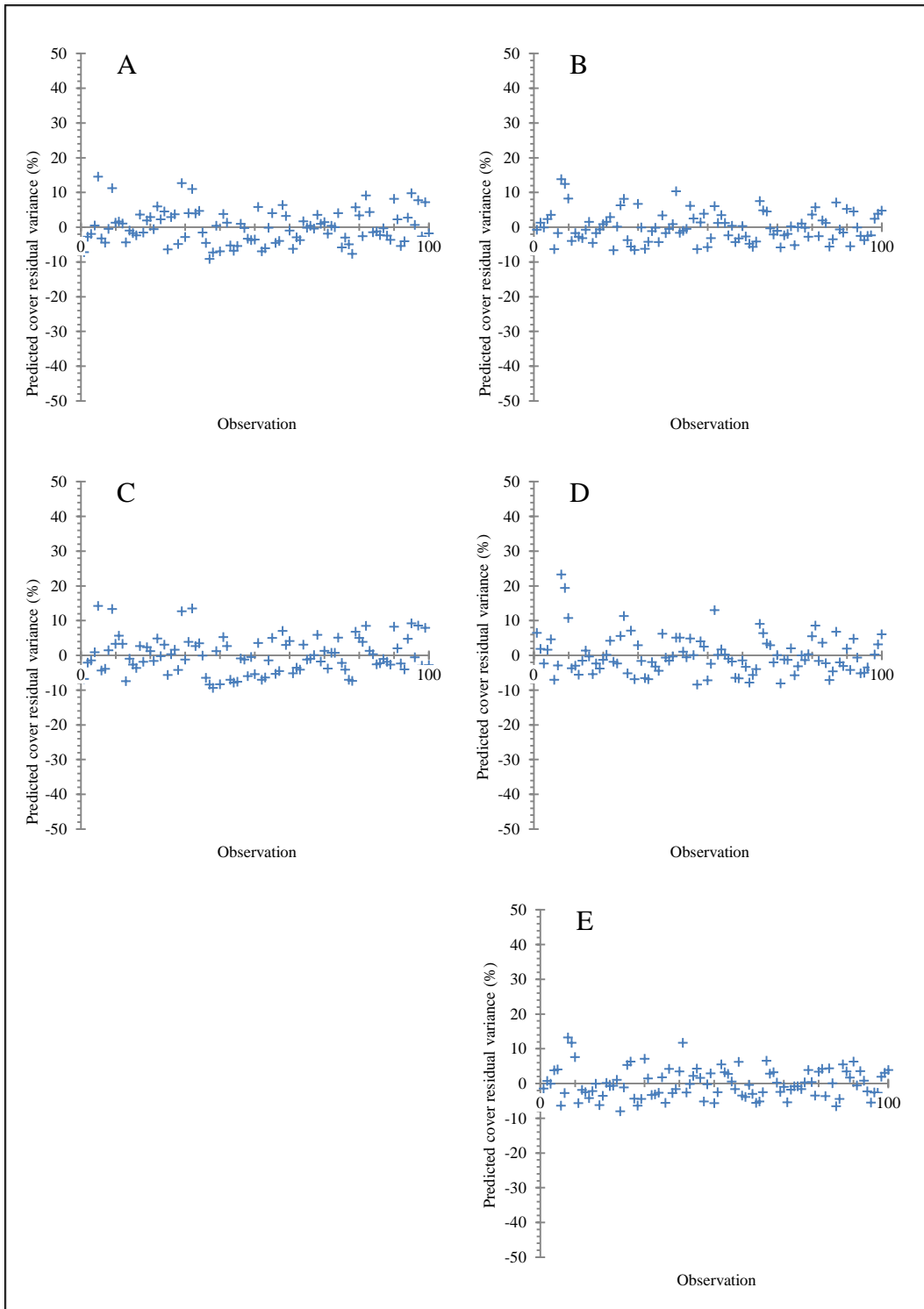


Figure 4.6 Residual variance figures for final mixed-cover by PC bands NDVI-EVI-RVI using: (A) 3x3 window and 30 m NAIP; (B) 3x3 window and 90 m NAIP; (D) 5x5 window and 90 m NAIP. Residual variance figures for PC bands NDVI-EVI-RVI-SAVI using: (C) 3x3 window and 30 m NAIP; (E) 3x3 window and 90 m NAIP. Note: These data have been calibrated by adding residual variance figures to modeled values in order to correct for systematic error.

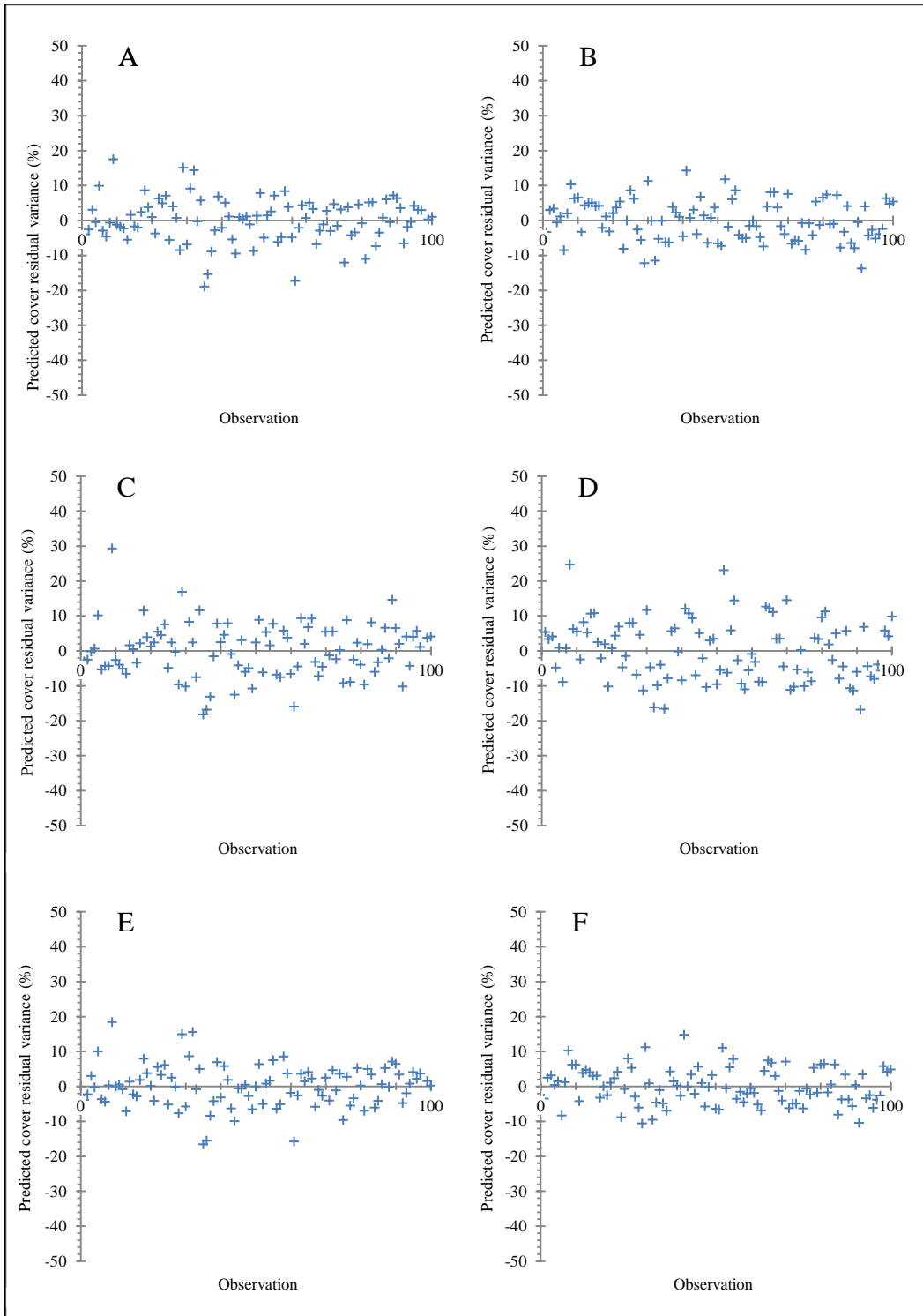


Figure 4.7 Residual variance figures for final coniferous-cover by PC bands NDVI-EVI-RVI using: (A) 3x3 window and 30 m NAIP; (B) 3x3 window and 90 m NAIP; (C) 5x5 window and 30 m NAIP; (D) 5x5 window and 90 m NAIP; Residual variance figures for PC bands NDVI-EVI-RVI-SAVI using: (E) 3x3 window and 30 m NAIP; (F) 3x3 window and 90 m NAIP. Note: These data have been calibrated by adding residual variance figures to modeled values in order to correct for systematic error.

CHAPTER 5

DISCUSSION AND CONCLUSIONS

5.1 Spectral Responses to Landscape Dynamics

The models developed in this study based on remote sensing slightly overestimated cover as determined on the ground. The models more accurately predicted percent-cover in the 3x3 local window than in either the 5x5 or 7x7 windows. Models built using three vegetation indices (NDVI, EVI, and RVI) were superior to those using all four vegetation indices (NDVI, EVI, RVI, and SAVI) as well as those that used all multispectral bands (bands 123457). In particular, models designed to predict forest percent-cover in coniferous and mixed coniferous/deciduous stands were more accurate than those designed for deciduous forest stands. Salvador and Pons (1998) also found this in a mixed pine and oak Mediterranean woodland.

5.1.1 Influence of Forest Structure on Data

Several inherent issues rest in the make-up of forest stand spectra characterized by complex open canopies and shadowing. In forests with relatively “open” canopies (i.e., sparse or low-density crowns), the spectral response of canopy cover may be blended with understory signals (Franklin et al. 2003, Smith et al. 2009, Welles and Cohen 1996), as groundcover vegetation inevitably confuses the reflectance signature of canopies within especially large-resolution locales. Open stands also allow the transmission of light to the lower layers of a tree, which obscures signatures as the muted signal received by a stand’s lower layers gives the impression of increased shadowing (Crist and Cicone 1986). This may especially be an issue with deciduous species, as the overlapping nature of foliage common to deciduous stands is more pronounced (Wulder 1998). Furthermore, shadowing becomes an issue in open forests as the sheer nature of the vertical distribution of foliage, as well as the gap size between trees, reduces illumination and specifically confuses the value of Landsat TM’s tasseled cap wetness band (band 3), as its sensitivity to shadows is interpreted as increased soil-moisture and vegetation density (Crist and Cicone 1986, Dymond et al. 2002), clarifying why the models may have over-predicted percent-cover. Horler and Ahern (1986) go further in their finding that PC band 3 coefficients are almost identical to those of TC band 3, creating similar issues. In turn, it may have been

advantageous to either remove the problem by subtracting shadows from the imagery prior to any analysis (Franklin et al. 1991, Huang et al. 2001, Wolter et al. 1995).

5.1.2. Regional Influence on Data and Indices

It is also suspected that the leaf-area-index value $L=0.5$, utilized in all EVI and SAVI models (see Table 3.3), may have created lofty estimates for the final simulations presented in this study. Huete (1988) and Liu and Huete (1994) advocate the value $L=0.5$ as an appropriate scaling factor for intermediate levels of cover, for the optimal value of “L” depends on vegetation density. When dealing with low-density levels, $L=1$ is suggested (and $L=0.25$ for high-density levels) (Huete 1988). Given that a southwestern stand may very well represent vegetation densities less than that of an “average” stand (located in a less-stressed environment), by using a higher scaling factor (such as $L=0.6$), the final models may have been better-suited for a more sparse cover (Huete 1988). Overall, this calibration may have resulted in a lower signal, thus more-accurate percent-cover predictions. Also, it may have been beneficial to account for such variability by stratifying the value of “L” into different classes based off of plot composition relevé charts.

Salvador and Pons (1998) explored the facility of combinations of TM bands 1, 2, 3, 4, 5, 7, NDVI, and a Modified Normalized Difference Vegetation Index (MNDVI; specialized for coniferous forests) in a heterogeneous Mediterranean landscape within both heterogeneous and homogenous vegetation plots. They found that by combining all of the above components, collinearity diminished. The most accurate index ($R^2 = 0.78$), tested within homogeneous stands of *Pinus sylvestris*, was the MNDVI (originally designed by Nemani et al. 1993). Though this index is based off of a study area located in a Pacific Northwest watershed, and designed to correct for understory spectra, it is possible this index may improve the accuracy of the models presented in this study, as it may after all be comparable to the Prescott area as it was comparable to a fairly similar Mediterranean landscape.

5.2 Examination of Techniques and Procedures

The forest canopy cover models presented in this study did simulate actual cover to a certain degree, however, some oversights exist. In hindsight, it is apparent that some changes in

data collection techniques and processing may be tweaked to refine the models and gain more accuracy.

5.2.1 Data Acquisition

Cover estimates generated with the vertical densitometer were collected in late 2008. The acquisition date of the imagery from which the models were built was in the spring of 2008. The acquisition date of the aerial imagery from which the accuracy of the models was tested was in the summer of 2007. Though the spans of time between these dates are minimal, they are not ideal. This may account for the models' over-estimation of cover, as the reference imagery (NAIP orthophoto) may not have captured canopies that were recorded roughly one year later in the field or by satellite. In addition, cover estimates, generated with the vertical densitometer, were determined by the percentage of cover directly overhead; by estimating what percentage of the instrument's field of view was obstructed. These readings excluded canopies less than 6 feet in height, thus such totals were absent from all final percent-cover totals.

5.2.2 Normalizing Cover

Because no plot accounted for 0% canopy cover, having no less than 2 trees intersect one of three transects, three additional pixels, or "pseudo-plots" (with exceptionally low digital values; nearly 0% canopy cover) were added to each dataset (see section 3.3.3). This reduced discontinuity and normalized the natural range of these data to provide the models with a baseline from which it could better identify patterns, however because these pixel values did not quite equal zero (i.e., "true black" or 0% cover), the models' percent-cover totals (i.e., pixel values) were slightly inflated. This may be another reason why the models over-predicted cover. Therefore, it may have been better to sample plots that expressed values across the entire spectrum of the ecology in question.

It is also possible that by using the pixel that intersected the lengthiest transect circumference, rather than the pixel with the most plot-pixel area coverage, the models would have been built with more precision, as the data paired with those pixels would have been more representative of actual cover given that the coefficients used to design the models were based solely on the relationship between those pixels and relative transect readings. In other words, the

training data for the models may have been better-fit had they been based on the pixel with the most information (i.e. forest percent-cover data), rather than the pixel with the most area.

5.3 Conclusions

The conclusions of this study are threefold:

1. The principal components of different composite bands and vegetation indices are an effective way to predict percent-cover. The most accurate combination of composites, vegetation indices, and band combinations incorporated the principal components of NDVI, EVI, and RVI. According to the final models, this particular combination of spectral transformations surpassed all other transformation combinations. In addition, the 90 meter orthophoto (as opposed to the 30 meter) contained less locational error.
2. The optimal window size for predicting percent-cover was the 3x3 moving window. Though the accuracy of models predicted with a 5x5 moving window were highly accurate, the 3x3 moving window proved to be more precise.
3. Percent-cover is best predicted for coniferous and mixed coniferous/deciduous forest stands. Deciduous forest percent-cover is more difficult to accurately predict.

REFERENCES

- Carreiras, J.M.B. et al. 2006. Estimation of tree canopy cover in evergreen oak woodlands using remote sensing. *Forest Ecology and Management*, 223, 45-53.
- Corwin, T. 2004. Creek Observation Guide. Prescott Creeks, Prescott Arizona.
- Crist, E.P. et al. 1986. Vegetation and soils information contained in transformed Thematic Mapper data. *Proceedings of IGARSS' 86 Symposium*, pp. 1465-1470.
- Crist, E.P. and R.C. Cicone. 1984. Application of the tasseled cap concept to simulated Thematic Mapper data. *Photogrammetric Engineering & Remote Sensing*, 50(3), 343-352.
- Dymond, C.C. et al. 2002. Phenological differences in Tasseled Cap indices improve deciduous forest classification. *Remote Sensing of the Environment*, 80, 460-472.
- Franklin, S.E. et al. 2003. Discrimination of conifer height, age, and crown closure classes using Landsat-5 TM imagery in the Canadian Northwest Territories. *International Journal of Remote Sensing*, 24(9), 1823-1834.
- Franklin, J. et al. 1991. Thematic Mapper analysis of tree cover in semiarid woodlands using a model of canopy shadowing. *Remote Sensing of Environment*, 36, 189-202.
- Horler, D.H.N. and F.J. Ahern. 1986. Forestry information content of Thematic Mapper data. *International Journal of Remote Sensing*, 7(3) 405-428.
- Huang, C. et al. 2001. A strategy for estimating tree canopy density using Landsat 7 ETM+ and high resolution images over large areas. *Proceedings of the Third International Conference on Geospatial Information in Agriculture and Forestry*, Denver, CO, November 5-7.
- Huete, A.R. 1988. A soil-adjusted vegetation index (SAVI). *Remote Sensing of Environment*, 25, 295-309.
- Jordan, C.F. 1969. Derivation of leaf-area-index from quality of light on forest floor. *Ecology*, 50(4), 663-666.
- Kaufman, Y.J. and D. Tanre. 1992. Atmospherically-resistant vegetation index (ARVI) for EOS-MODIS. *IEEE Transactions on Geoscience and Remote Sensing*, 30(2), 261-270.
- Kauth, R.J. and G.S. Thomas. 1976. The Tasseled Cap - a graphic description of the spectral-temporal development of agricultural crops as seen by Landsat. *Proceedings of a Symposium on Machine Processing of Remotely Sensed Data*, Purdue University, West Lafayette, IN, June 21 – July 1, pp. 4B41-4B51.
- Kriegler, F.J. et al. Preprocessing transformations and their effect on multispectral recognition. *Proceedings of the sixth International Symposium on Remote Sensing of Environment*, University of Michigan, Ann Arbor, MI, pp. 97-131.
- Lillesand, T.M. and R.W. Kiefer. 1972. *Remote Sensing and Image Interpretation*. John Wiley and Sons, Second Edition, pp. 721.
- Liu, H.Q. and A. Huete. 1995. A feedback based modification of the NDVI to minimize canopy background and atmospheric noise. *IEEE Transactions on Geoscience and Remote Sensing*, 33(2), 457-465.

- Myint, S.W. 2010. Multi-resolution decomposition in relation to characteristic scales and local window sizes using an operational wavelet algorithm. *International Journal of Remote Sensing*, 31(10), 2551-2572.
- Rouse, J.W. et al. 1973. Monitoring vegetation systems in the Great Plains with ERTS-1. *Third Earth Resources Technology Satellite Symposium*, pp. 309-317.
- Ryberg, E. 2008. A living dinosaur in Prescott. *Prescott AZ News and Events – Read It Here Magazine*.
http://www.readitnews.com/index.php?option=com_content&task=view&id=47 (last accessed 3 September 2011).
- Ryberg, E. 2005. Monarchs of the forest. *Arizona Wild: Newsletter of the Arizona Wilderness Coalition*. <http://www.azwild.org/newsletter/documents/AZWILD1105.pdf> (last accessed 14 October 2010).
- Salvador, R. and X. Pons. 2006. On the applicability of Landsat TM images to Mediterranean forest inventories. *Forest Ecology and Management*, 104, 193-208.
- Shalau, J. 2003. Ponderosa Pine Bark Beetles in the Prescott Area. *The University of Arizona cooperative extension research reports – Yavapai County*.
ag.arizona.edu/yavapai/anr/fh/PrescottBarkBeetles.pdf (last accessed 14 February 12).
- Smith, A.M.S. et al. 2009. A cross-comparison of field, spectral, and lidar estimates of forest canopy cover. *Canadian Journal of Remote Sensing*, 35(5), 447-459.
- Southwest Environmental Information Network (SEINet). 2011. Yavapai County public survey checklist. <http://swbiodiversity.org/seinet/checklists/survey.php?surveyid=62> (last accessed 11 Feb 2011).
- Stumpf, K.A. 1993. The estimation of forest vegetation cover descriptions using a vertical densitometer. A paper presented at the joint Inventory and Biometrics Working Groups session at the SAF National Convention, Indianapolis, IN, on November 8–10.
- Tomlinson, J.R. et al. 1999. Coordinating methodologies for scaling landcover classifications from site-specific to global: Steps toward validating global map products. *Remote Sensing of Environment*, 70 (16-28).
- U.S. Forest Service. 2006. *About Prescott National Forest*.
<http://www.fs.fed.us/r3/prescott/about/index.shtml> (last accessed 23 September 2009).
- U.S. Forest Service. 2011. *Bark beetle removal projects*. <http://www.fs.fed.us/r3/prescott/forest-health/beetle-points.shtml> (last accessed 14 February 2012).
- Welles, J.M. and S. Cohen. 1996. Canopy structure measurement by gap fraction analysis using commercial instrumentation. *Journal of Experimental Botany*, 47(302), 1335-1342.
- Wolter, P.T. et al. 1995. Improved forest classification in the northern lake states using multi-temporal Landsat imagery. *Photogrammetric Engineering and Remote Sensing*, 61(9), 1129-1143.
- Wulder, M. 1998. Optical remote-sensing techniques for the assessment of forest inventory and biophysical parameters. *Progress in Physical Geography*, 22(4), 449-476

